MODELING AND ANALYSIS OF A ROBOTIC ARM FOR ARC AND SPOT WELDING

Dissertation submitted

in partial fulfillment for requirements

for the award of degree of

Bachelor of Technology

in

Mechanical Engineering

by

P. PURUSHOTHAM	**15131A03E3**
R. RAJU	**15131A03F8**
N. VAMSI KRISHNA	**15131A03B9**

Under the guidance of

Dr. K. V. Vara Lakshmi

Assistant Professor

Department of Mechanical Engineering

Department of Mechanical Engineering
GAYATRI VIDYA PARISHAD COLLEGE OF ENGINEERING
(AUTONOMOUS)
(Affiliated to J. N. T. University, Kakinada)
VISAKHAPATNAM-530048

2015-19

MODELING AND ANALYSIS OF A ROBOTIC ARM FOR ARC AND SPOT WELDING

Dissertation submitted

in partial fulfillment for requirements

for the award of degree of

Bachelor of Technology

in

Mechanical Engineering

by

P. PURUSHOTHAM	**15131A03E3**
R. RAJU	**15131A03F8**
N. VAMSI KRISHNA	**15131A03B9**

Under the guidance of

Dr. K. V. Vara Lakshmi

Assistant Professor

Department of Mechanical Engineering

Department of Mechanical Engineering
GAYATRI VIDYA PARISHAD COLLEGE OF ENGINEERING
(AUTONOMOUS)
(Affiliated to J. N. T. University, Kakinada)
VISAKHAPATNAM-530048

2015-19

DECLARATION

We hereby declare that the project entitled "**MODELING AND ANALYSIS OF A ROBOTIC ARM FOR ARC AND SPOT WELDING"** submitted by us, for the award of the Degree of Bachelor of Technology in Mechanical Engineering to Gayatri Vidya Parishad College of Engineering (A) is a bonafide record of our work carried out under the supervision of Dr. K. V. Vara Lakshmi.

We further declare that the work reported in this project has not been submitted and will not be submitted, either in part or in full, for the award of any other degree or diploma in this institute or any other institute or university.

CERTIFICATE

This is to certify that the project titled "**MODELING AND ANALYSIS OF A ROBOTIC ARM FOR ARC AND SPOT WELDING**" is a bonafide record of the work done by

P. PURUSHOTHAM	**15131A03E3**
R. RAJU	**15131A03F8**
N. VAMSI KRISHNA	**15131A03B9**

in partial fulfillment of the requirements for the award of the degree of **BACHELOR OF TECHNOLOGY IN MECHANICAL ENGINEERING of** Gayatri Vidya Parishad College of Engineering (Autonomous) affiliated to Jawaharlal Nehru Technological University, Kakinada during the year **2015-19.**

Project Guide	**Head of the Department**
Dr. K. V. Vara Lakshmi **Assistant Professor,** **Dept. of Mechanical Engineering**	**Dr. B. Govinda Rao** **Professor and HOD,** **Dept. of Mechanical Engineering**

Project Viva – Voice held on

External Examiner

ACKNOWLEDGEMENT

It is with a sense of great respect and gratitude that we express our sincere thanks to Dr. K. V. Vara Lakshmi, Assistant Professor, Department of Mechanical Engineering, Gayatri Vidya Parishad College of Engineering (A) for her inspiring guidance, supervision, and encouragement towards the successful completion of our project work.

We take this opportunity to thank Dr. B. Govinda Rao, Professor and Head of the Department of Mechanical Engineering, for permitting us to pursue the project work.

We express our sincere thanks to Dr. A. B. Koteswara Rao, Principal, Gayatri Vidya Parishad College of Engineering (A) for granting permission for providing all the necessary resources for completing this project.

We wish to express our appreciation and heartful thanks to our parents who supported us towards our goals and we would like to thank our friends, who have helped us and inspired us in odd and even hours for the successful completion of project work.

Last but not the least, we would like to convey special thanks to all those to who have helped either directly or indirectly for the completion of project work.

ABSTRACT

Robotic arms are extensively used in industries for its precise work and reduced time for manufacturing a product. In industries, robotic arms are used for various applications like CNC lathe, assembling, painting, welding etc., In this project, a 6-degrees of freedom (DOF) robotic arm with two different grippers are modeled. The aim of this project is to design a robotic arm is to be fixed on the roof top in an industry to increase the work environment. A scaled model of a 6-DOF industrial serial robotic arm is considered for the design and analysis. For the designed model, the forward kinematic analysis is done using D-H notations for the kinematic simulation and workspace analysis. The robotic arm is used for spot and arc welding, grippers are designed and simulated to get desired output. To know the behavior of the robotic arm static, dynamic and modal analysis will be performed.

CONTENTS

List of Tables

List of Figures

1 Introduction

Robotics can be described as the current pinnacle of technical development, using the continuing advancements of mechanical engineering, material science, mechatronic systems, manufacturing techniques, and advanced algorithms. Robotics can be defined as the science or study of the technology primarily associated with the design, fabrication, theory, and application. In other words, a robot is a machine designed to execute one or more tasks automatically with speed and precision. A robot is a machine which can be controlled either by embedded algorithm or by giving an external input to do various tasks.

An industrial robot system used for manufacturing which are automated, programmable and capable of movement on three or more axis. In industries there are various kinds of tasks that are being accomplished by robots like performing material handling, welding, assembly, pick and place operations, painting, milling operations, etc., Robots used in industries are called industrial robots which have high precision and can perform tasks which involve more labour-intensive work. In the year 2015, an estimated 1.64 million industrial robots were in operation worldwide according to International Federation of Robotics. Based on the requirement, there are few types of industrial robots were developed. They are Cartesian, SCARA, Delta, Polar, KUKA, PUMA and various other kinds of robots with different types of joint movement or gripper to perform different tasks. Many industrial robots are having an arm called robotic arm with various revolute and linear joints which also have different degrees of freedom (DOF).

Table 1-1 Types of robotic arm and its applications

Type of robot	Application
Cartesian (Cartesian Co-ordinate robot, moves in straight lines, 3-DOF)	Used in CNC lathes
SCARA (Selective Compliance Articulated Robot arm, 6-DOF)	Pick and Place operation or Assembly operations
KUKA (Keller und Knappich Augsburg, 6-DOF)	Welding operations, Machining and Forging
PUMA (Programmable Universal Machine for Assembly,6-DOF)	Assembly operations

Degrees of freedom (DOF) is defined as the number of independent ways by which a dynamic system can move, without violating any constraint imposed on it, is called number of degrees of freedom. In other words, the number of degrees of freedom can be defined as the minimum number of independent coordinates that can specify the position of the system completely.

1.1 Background: Anatomy of Robots

The mechanical structure of a robot is like skeleton in the human body which is having a robotic arm called manipulator. Robot anatomy is the study of skeleton of the robot i.e., physical construction of the manipulator. The mechanical structure in a robot consists of rigid bodies like links which are connected by means of articulations called joints, is segmented into an arm that can be used for mobility. A wrist that confers orientation and an end-effector that performs the required task. Most manipulators are mounted on the base of a floor or on the mobile platforms of an autonomous guided vehicle (AGV).

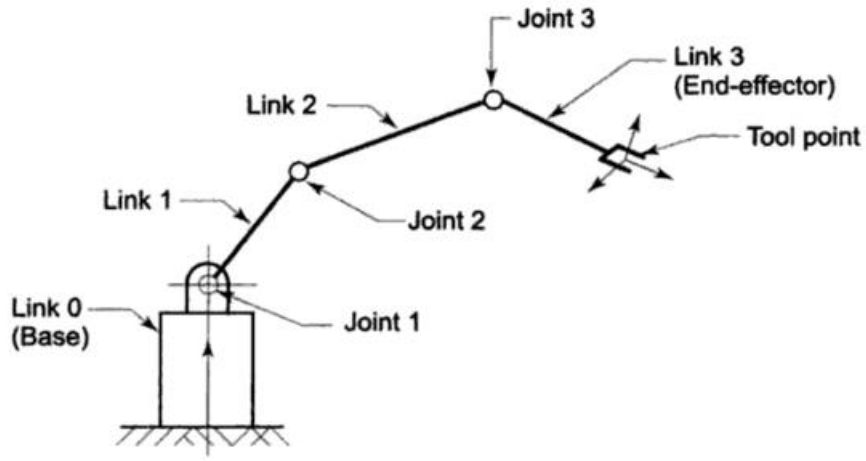

Figure 1-1 Structure of Robotic arm

The manipulator of an industrial robot consists of a series of joints and links shown in Fig 1-1, which are called serial manipulators. A robotic joint provides relative motion between two rigid links that can be connected with each other and form a binary link. Joint provides controlled relative movement between the input link and output link. Each joint, or axis, provides a certain degree-of-freedom (DOF) of motion. In most of the cases, only one degree-of-freedom is associated with each joint. Therefore, the robot's complexity can be classified according to the total number of degrees-of-freedom they possess. Each joint and each links are named in a scheme that begins from

the bottoms of the robotic arm, first link is named as link-0, and second link as link-1 and joints are named as first joint is Joint-1, second Joint-2 as shown in the Fig. 1.2.

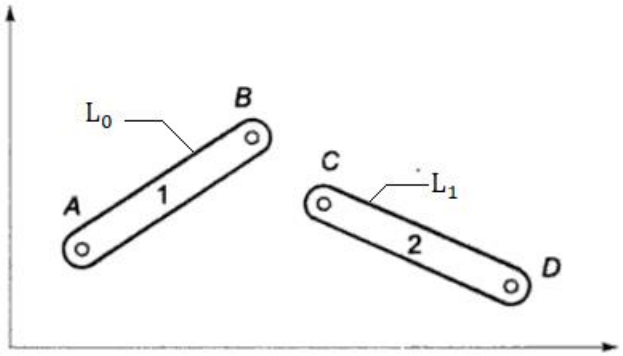

Figure 1-2 Representation of joints and links

1.1.1 Types of Joints

Joints represent the movement of any two links with respect to the co-ordinate axis. The following Table 1.2 describes about various joint movements.

Table 1-2 Types of joints present in a Robotic arm

Name of Joint	Description
Revolute	Allows relative rotation about one axis.
Cylindrical	Allows relative rotation and translation about one axis.
Prismatic	Allows relative translation about one axis.
Spherical	Allows three degrees of rotational freedom about the centre of the joint. Also known as a ball-and-socket joint.
Planar	Allows relative translation on a plane and relative rotation about an axis perpendicular to the plane.

1.1.2 Joints used for arc and spot-welding in robotic arm

There are mainly two types of joints that can be established between two links which are

- Revolute (R)
- Prismatic (P)

The relative motion of each joint between the two links is either rotational movement or translational movement. A revolute joint also called pin joint or hinge joint is a one degree of freedom kinematic pair used in mechanisms. Revolute joints provide single-axis rotation function used in many places such as door hinges, folding mechanisms, and other uni-axial rotation devices.

A prismatic joint provides a linear sliding movement between two bodies, and is often called a slider, as in the slider crank linkage. A prismatic pair is also called as sliding pair. In the following Fig. 1.3, three linear joints i.e., T_1, T_2, T_3 and three revolute joints R_1, R_2, R_3 are shown in joint co-ordinate axes.

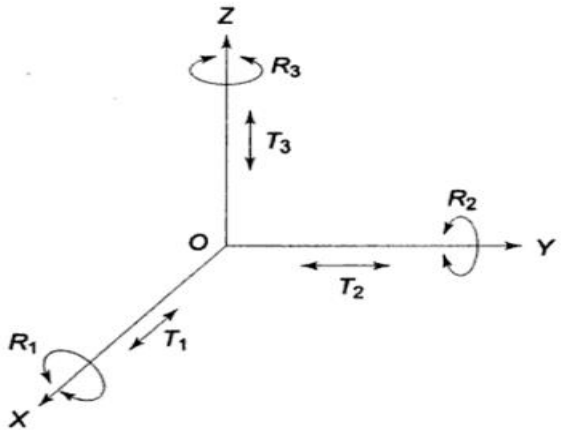

Figure 1-3 Joint coordinates axes

1.1.3 Arm Configuration

A robotic arm consists of various links and joints which makes the manipulator to position the wrist in the required co-ordinates. The number of degrees of freedom depends on the type of joints employed. If a robot is having one revolute joint and one prismatic joint it is having 2-DOF. The number of degrees of freedom depends on the type of shape that the robotic arm can sweep. There are four general configurations as shown in Table 1.3.

Table 1-3 Types of Robotic arm Configuration

Type of Configuration	Type of Joint	Number of DOF
Cartesian configuration	3 Prismatic joints	3 degrees of freedom
Cylindrical configuration	1 Revolute joint and 2 Prismatic joints	3 degrees of freedom
Polar configuration	2 Revolute joints and 1 Prismatic joint	3 degrees of freedom
Articulated configuration	3 Revolute joints	3 degrees of freedom

1.2 End-Effectors

End-Effector in a robotic arm is designed to interact with the environment which is a device placed at the end of the robotic arm. At the end point various tools are attached

according to the type of application. The end-effector may consist either tools or grippers attached at the end of the serial manipulator.

Grippers are used to hold the work piece or objects in an industry used for pick and place operation and other assembly of products, they are like human fingers which are used to grab objects. The applications include material handling, machine loading and unloading, pelleting, and other operations. There are few types of grippers which are used in any industry.

- Mechanical
- Magnetic
- Vacuum cups
- Bellows
- Hydraulic grippers

A mechanical gripper is used as an end effector in a robot for grasping the objects with its mechanically operated fingers. In industries, two fingers are enough for holding purposes. More than three fingers can also be used based on the application. As most of the fingers are of replaceable type, it can be easily removed and replaced.

A robot requires either hydraulic, electric, or pneumatic drive system to create the input power. The power produced is sent to the gripper for making the fingers react. It also allows the fingers to perform open and close actions. Most importantly, a sufficient force must be given to hold the object.

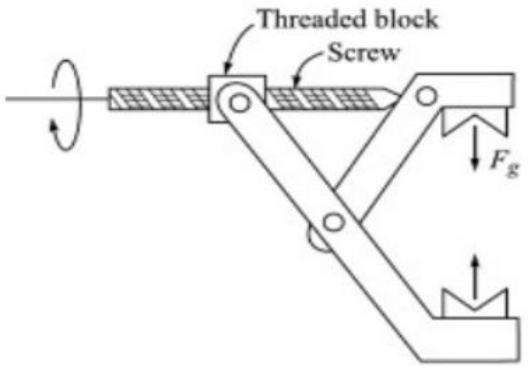

Figure 1-4 Mechanical Gripper

Magnetic grippers having a magnetized element which is used to hold the objects which are ferro-magnetic in nature such as steel, blanks, stamped parts and can also use for cleaning the chips from machining operations. For maximum holding force

in extremely confined spaces. When using ferromagnetic workpieces requires maximum holding forces in extremely confined spaces, magnetic gripping is the ideal solution.

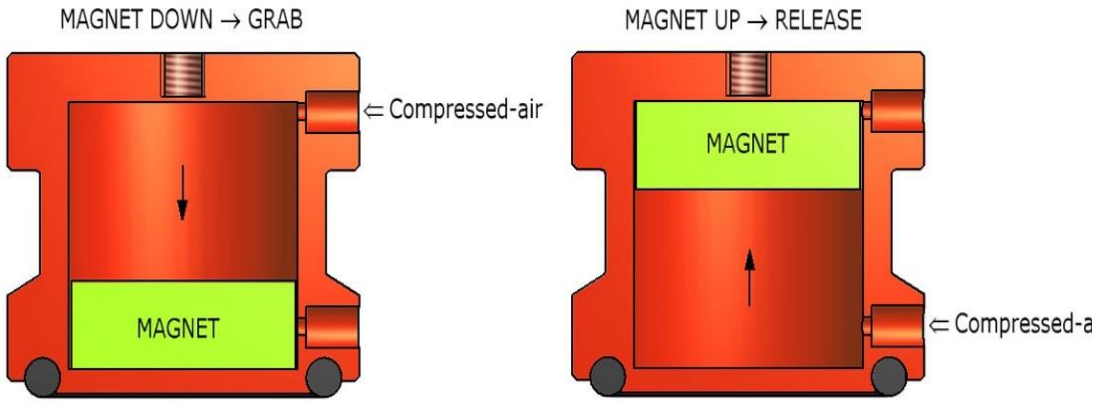

Figure 1-5 Magnetic Gripper

Vacuum grippers or vacuum cups have a cup design to hold any object using the vacuum suction created. These grippers are mainly used for light weight objects holding and transferring. Very less amount of gripping force is created used for transferring mirrors, glass plates etc.,

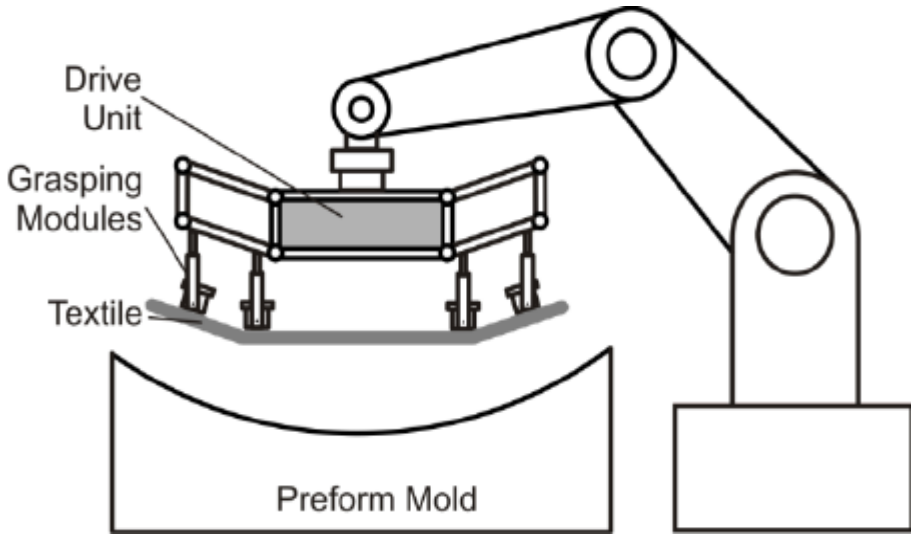

Figure 1-6 Vacuum grippers

The end-effector may also have tools at the end point for various operations like welding, machining, forging, lathe machining etc.,

1.3 Degrees of freedom

The degrees of freedom of a serial manipulator can be obtained from the well-known Chebychev Grubler-Kutzbach criterion,

$$\text{DOF} = \lambda\,(\text{N} - \text{J} - 1) + \sum_{i=1}^{J} F_i \tag{1.1}$$

The quantity, DOF, obtained from Eq. (1.1) is the number of independent actuators that can be present in the serial manipulator. In a broad sense, DOF determines the capability of the serial manipulator with respect to dimension of the ambient space λ. We have the following possibilities:

1. DOF = λ – In this case, an end-effector of a manipulator can be positioned and oriented arbitrarily in the ambient space of motion.

2. DOF < λ – In this case, the arbitrary position and orientation of the end-effector is not achievable and there exist (λ − DOF) functional relationships containing the position and orientation variables of the end-effector.

3. DOF > λ – These are called redundant manipulators and the end-effector can be positioned and oriented in infinite number of ways. In serial manipulators with a fixed base, a free end-effector and two links connected by a joint, from Eq. (1.1), N = J + 1 and

If all the actuated joints are one- degree-of freedom joints, then J = DOF. If J <DOF, then one or more of the actuated joints are multi- degree-of-freedom joints and this is not used in mechanical serial manipulators. This is due to the fact that it is difficult to locate and actuate two or more one- degree-of-freedom joints at the same place in a serial manipulator.

1.4 Advantages of robotic arms

- Due to its mechanical nature and computerized control, a robotic arm can carry out a repetitive task with great precision and accuracy.
- Efficiency and production rate increases.
- Eliminates dangerous working condition for workers near high temperature working conditions.
- Reduce amount of operator errors.

- Easily programmable to do any task and easy to control the work from remote locations.

1.4.1 Disadvantages of robotic arms

- High standards of maintenance are required.
- Time, training and specialized workers needed for programming various tasks.
- Complex to install and expensive in cost.
- A skilled operator required even few robotic arms are fully automated.

1.5 Literature Review

The following works are related to the present thesis:

Fleischer et al. [1] studied on Automated Analytical Measurement Processes Using a Dual-Arm Robotic System. Bio-screening and high throughput and high-content screening processes, analytical measurement procedures are complex in their structure and changing frequently. The transportation or specific single tasks, but also flexible robots are needed to cover several tasks, including transportation and direct sample manipulation. Due to their human-like structure, dual-arm robots are predestined for analytical measurement processes, energies present a novel integration of electronic piston pipettes into an automation system using a dual-arm robot to perform liquid handling tasks similar to human operators. Analytical measurements are developed and analyzed their orientation which improved their flexibility a lot when compared to a normal model.

EL Daou et al. [2] developed an experimental protocols of robotic hip joint. The implementation of optical tracking and registration techniques of the hip joint center of rotation (COR) in the coordinate system of the end-effector. This COR was used as the origin of the task related coordinate system whose axes are co-axial with the coordinate frame with a hybrid position to simulate tests. In comparison with an existing mechanical model of robotic systems developed a substantial improvement in terms of ability to position the hip joint.

Koivumaki et al. [3] discussed about the energy effective and high precision control of robot arm using hydraulics, in addition to high precision closed-loop control. The possibility for energy consumption reduction is realized by using a separate meter-in separate meter-out (SMISMO) control set-up, enabling an independent metering of

each chamber in hydraulic actuators. They have designed a subsystem-dynamics-based and modular controller for multiple degrees-of -freedom. SIMSMO-control methods are used for determining the motion and chamber pressure tracking performance. By using SIMSMO-control methods, the energy consumption is reduced by 45% without noticeable motion control.

Cruz et al. [4] studied about the twisting control for robotic arm. The control of industrial robotics systems is important due to the wide range of their applications. It is essential that the robot programmers can test the behavior of the robots in different circumferences and with varying parameters under a control methodology. A controller is designed based on 'Super Twisting Algorithm' robust nonlinear controller to reduce the chattering problem of sliding mode control. The simulated results are shown, compared with the proportional-derivative controller using the 5-DOF (degree of freedom) robotic manipulator.

Celikag et al. [5] studied the Stiffness optimization for Serial robots using cartesian stiffness model. It is necessary for development of proper stiffness and dynamic models is crucial to predict and compensate the tool deflections under cutting forces. This can be achieved by utilizing the functionally redundant degree of freedom (DOF) around the tool axis can vary by between 58% and 161% simply by utilizing the redundant degree of freedom of the robot. The stiffness of a serial arm robot was optimized to minimize the possible deflections during a milling operation. Finally, the work in this paper shows that there is a significant increase in the stiffness of the robot can be obtained by using this Cartesian Stiffness model.

Oaki [6] studied about the physical parameters estimation for controlling of the robotic arm. The model consists of fast and exact control of trajectory with elastic joints. A scheme used is torsion-angular velocity feedback (TVFB) scheme for suppressing residual vibration of the tip. The scheme utilizes a simple non-linear observer based on a physically parameterized dynamic model. The model consists of two-link robotic arm with elastic joints that are serially connected. The vibrations produced due to the coupled links of two-link joint which can be reduced through the feedback and feedforward control experiments and validated the effectiveness of the model using two-link robot arm.

Raza et al. [7] studied about kinematic analysis of an industrial robot and discussed about Geometrical improvement of a robotic arm. The proposed robotic arm is modeled using CAD software and analyzed the manipulator with structural and dynamic analysis. Inverse kinematic model is used to identify position of the gripper is identified. For developing the model of robot arm, ANSYS and SOLID WORKS software's were used. The data is used and industrial robot arm is developed.

Shanta and Azlan [8] studied the Sliding mode controller of robotic arm. The controlling of robotic arm is really challenging due to the involvement of various uncertainties such as time varying payload, friction and disturbances. These challenges attract many researches to develop advanced control strategies for robot arm. The formulation of a new Sliding Mode Control-Function Approximation Technique (SMC-FAT) based on the adaptive controller for a robot arm carrying unknown time-varying uncertainty is solved using FAT expression. The results with error less than 0.02 percentages proved the effectiveness of the proposed controller.

Kousi et al. [9] discussed about an outlook on the future assembly robotic arm workers. This paper investigates the effect of introducing mobile dual arm coworkers in manual assembly systems. The preliminary analysis indicates that with the proper re-assignment of roles between robotic and human resources can lead to significant enhancement in the operator working conditions, maintaining at least the same production levels as the current practice. Finally, the findings show that a significant increase in the resource's utilization can be achieved.

Pradhan et al. [10] implemented and evaluated a 4-degree of freedom (DOF) Selective compliance Assembly Robot Arm (SCARA). The design of SCARA is modeled in CAD software and controlling of movement using ACE controller. The entire model is implemented in a workspace area of 980 mm x 910 mm. Comparison of time saving and performance has been done between previous and implemented method shown as 50% reduction on time basis. Better results have been achieved on the basis of productivity increase, quality improvement

Brunot et al. [11] studied the state space estimation method for the identification of industrial robotic arm. The identification technique of model parameters and joint angles is conducted usually with Least-Square method which requires a careful preprocessing of data obtained of the dynamic parameters. The preprocessing mainly

consists of estimation of joint accelerations and velocities from the measured joint positions. There are few issues like pre-filtering to deal with closed-loop when using usual method. A new procedure based on Kalman filtering which is compared to usual method with experimental data considering an industrial robotic arm. The obtained results show that the proposed technique is a credible alternative.

Busson et al. [12] discussed about the task-oriented rigidity optimization of a 7-degrees of freedom (DOF) robot arm during tasks requiring stiffness. The Cartesian model reflected rigidity over an analytically computed manipulator which showed a significant- variations that require a right set of joint angles. Various experimental studies on a 7-DOF KUKA robot showed the relevance joint angles in finding the required angles which satisfies the rigidity criteria. The analytically computed cartesian model is optimized and also identified joint stiffness model of robot arm. The proposed approach can give efficient and convenient way to select the joint configuration of 7-DOF manipulator.

Marwan [13] discussed about the calibration is technique used to increase system positioning accuracy. The proposed technique is using an inertial measurement unit (IMU) to measure robot. The advantages of this method in comprising with the vision-based calibration, is that it does not need complex steps, such as camera calibration, image processing, memory and corner detection. The capability of the manipulator is increased in position and orientation and closed loop control. In comparison, the online calibration takes lesser time and close-loop control higher accuracy.

Hamaya et al. [14] developed exoskeleton robots in assistive strategies is a key ingredient. The interaction between users and exoskeleton robots in assistive strategy for bidirectional, designed complex and challenging solutions. The method used is 1-DOF exoskeleton robot and conducted a series of experiments are demonstrated as bi-directional interactions between a user and robot with only 60 seconds of interaction using human subjects. The proposed method enables a redundant robot arm to track a specified end-effector trajectory using a gesture which closely resembles human motion.

Bozek et al. [15] analyzed the dynamics model of a hexa-copter equipped with a robotic arm has been formulated using Newton– Euler's method and its stability was investigated. The discussion of the determination of the moment of inertia by simplified

pendulum method, in addition to taking into consideration the effects of mass distributions and CG change. A real and complex dynamic model was considered, which addresses the nonlinearity, time variance, under actuation, and disturbance. The model was created and developed various equations using SolidWorks and LabVIEW using Runge– Kutta 2 method and found that correlations were analyzed for all parameters of motion equations.

Fan et al. [16] proposed the optical flow and principal component analysis followed independent component analysis are combined for monitoring the motion process of robotic-arm-based system. Two kinds of optical flow, DOF and SOF, are employed as the samples which are created using computational fluid dynamics (CFD) of motion-related variables for forming models of DOF-PCA-ICA and SOF-PCA-ICA the proposed monitoring approaches are applied to monitor robotic-arm-based spray marking system. Compared to SOF-PCA-ICA, the DOF-PCA-ICA model is more accurate but consumes more time and memory space. So, when accuracy is most important index, we should choose DOF-PCA-ICA model.

Cen and Melkote [17] analyzed robot structural dynamics on the forces produced in robotic milling. The force model employs dynamic modeling of milling forces where the influence of system compliance on the equilibrium. The effect of milling forces on the robot arm stiffness is accounted for using the Conservative Congruence Transformation (CCT). Robotic milling experiments show around 50-60% reduction. The method accounts for the effect of robot structural vibration on the equilibrium or steady state uncut chip thickness of robot stiffness via the CCT-based robot stiffness model. Using this model, the arm configurations where the dynamic effect must be considered to reduce significant errors.

Yang et al. [18] developed an ultrasonic robotic system for small object manipulation which is capable of noncontact operation, remote control, and gesture-based intelligent control. The whole setup is composed of acoustic levitation platform, mobile operation platform, and Kinect sensing system which provides a humanized approach for human–machine interaction. The experimental results used for remote control of this acoustic levitation system based on gesture recognition method. The experiment results exhibit that remote noncontact operation with polystyrene beads was realized with our setup. the setup has been successfully built to manipulate the small objects in vertical direction by gesture.

Gutiérrez et al. [19] studied about designing a lightweight model of a robotic arm. The main objective is to reduce weight as well as to manufacture in low possible cost. The prototype is tested and fixed few elements for driving and controlling various links and joints. During the development of the prototype, several tests and studies such as strength simulation, dimensional effects and adjusted the control parameters to improve the accuracy testing of behavior of transmissions using Ansys and Matlab workbench. The prototype is a low- weight, and the overall performance of the manipulator is improved in accuracy, testing of behavior of transmissions.

Freddi [20] presented the redundancy analysis of two cooperative redundant manipulator through the use of the relative Jacobian matrix. The kinematic redundancy can be resolved by applying the principal local optimization techniques. This manipulator is kinematically redundant when the number of its possible motions n degree of motion is higher than the number of variables. Due to the presence of the Jacobian null space technique which presents a relevant computing effort, and thus a less computationally demanding control scheme, the implementation on a real controller of two anthropomorphic manipulators most suitable in the AAL scenarios is done with help of this method.

McMorran et al. [21] developed a flexible Selective Compliance Assembly Robot Arm (SCARA) which provide adaptability to serve and special applications in bio-chemical industry. A low-cost selective compliant articulated robotic arm designed using matlab for avoiding spillage of liquids. The construction of SCARA comprises aluminum brackets, aluminum tubing and hubs, injection-molded components, and custom-cut Lexan components. The Lynxmotion method of robotic arm was used under 4 degrees of freedom (DOF) to simplify understanding, the z axis is chosen to lie along the joint axis of each joint. Using a calculation method developed, it was possible to chart the regions where the obstacle was likely to be located when a collision occurred.

Li et al. [22] discussed about grasping posture control for a robotic arm is developed based on novel adaptive particle swarm optimization (PSO) for the home service robot. The coordinate system of the 6-DOF robotic arm can be divided into four parts shoulder, elbow, wrist and hand, as shown using Denavit–Hartenberg (DH) method. The algorithm used for comparisons of simulation results among ABC, GABC, LHNPSO, OTIWPSO, AIWPSO, AIWCPSO and AIWCPSO-S algorithms,

AIWCPSO-S can solve the problem of grasping posture control for the 6-DOF robotic arm. Lastly, through real-time experiments on the 6-DOF robotic arm, the grasping posture control can be successfully accomplished.

Roy et al. [23] studied about the trajectory path planning of EEG controlled robotic arm used to control artificial arm which can help people with disability to interact with their physical environment. EEG data for motor imagery were captured from five healthy subjects and left-right hand movement was classified using support vector. A trajectory path for an EEG controlled robotic arm, 75.77% classification accuracy is obtained for the left-right arm movement. Using this method, we could simulate human hand kinematics with higher DOF. Thus, GA based EEG controlled robotic arm could be used for real time applications.

Al-Junaid [24] proposed a robotic arm which has visual servoing systems in this paper. The manipulator is based on ANN mechanism to model inter-related visual kinematic relations. Arm movements, dynamics, and kinematics were simulated with Matlab robotics tool. The arm is equipped with a CCD camera, where the visual CCD part is modeled and simulated with Matlab Epi-polar Geometry Toolbox. ANN with an image based visual servoing system. A four layers ANN is used to learn a 6 DOF robotic arm kinematic relations described by a scene feature Jacobian based on epi-polar geometry based visual servoing. ANN was also able to learn the complicated kinematics visual relations relating the closed loop movement using this methodology.

Bouzgou and Ahmed-Foitih et al. [25] studied the criteria for choosing the best solution among the solutions of the inverse geometric model of the 6 degrees of freedom (DOF) robot arm. The model of a 6- DOF is designed and simulated using CAD. The model is analyzed using inverse kinematics which gives us the nonlinear equation for find the singular configurations in Matlab. The inverse kinematic model gives us the eight solutions of the positions of the end-effector apart from the singularities, validation is done using a virtual environment software. In among 8 results generated in virtual environment, a desired workspace area is selected for the 6-DOF robotic arm.

Sunny et al. [26] studied about robotic arm with a brain computer interfaces (BCI), is a modern technology which is currently revolutionizing the field of signal processing. BCI helped in the evolution of a new world where man and computer had never been so close. Electroencephalography (EEG), which is the measurement and recording of

electric signals using sensors arrayed across the scalp conditioning and processing. A low-cost system implementation that can even serve as a reliable substitute for the existing technologies of prosthesis like BIONICS. The same technology can be extended to develop a brain controlled robotic leg which can also serve as a prosthetic appendage for physically challenged.

Jobbagy et al. [27] studied about artificial muscles which they have discussed about application of robotic arm and rehabilitation process. The robot-assisted rehabilitation of the upper limb where is also described an architecture of robotic rehabilitation and its main functions are discussed and exhibited various results. The design of robotic arm with artificial muscles for rehabilitation of the upper limb is carried on Catia and Ansys also for analyzing the stress-strain parameters. The data collected from Ansys is analyzed with the help of kinematic equations and the results shows that the model with artificial muscles can with-stand more load than a normal robot manipulator.

Lin et al. [28] analyzed the kinematic control of a robot arm to track a specified end-effector trajectory is achieved. But the proposed robotic arm cannot be controlled dynamically. To improve intuitive control, this work proposes a novel method to control with divergence problems of previous multi-tasking methods when human motion is applied. Various simulations with a redundant robot arm is used to validate the proposed kinematic-control method. The proposed method enables a redundant robot arm to track a specified end-effector trajectory using a gesture which closely resembles human motion which is analyzed and improved in precision and control.

Gomez-Espinosa [29] designed a 3-DOF parallel links robot, and proposed a didactic platform using methodology for allowing different manufacturing processes and robot architectures to be incorporated and the available tools and facilities. kinematic and dynamic analysis of further application development for easier peripheral implementation such as with video cameras or voice recognition. The sub-assemblies of the mechanisms are analyzed, main technical areas and their processes are discussed individually emphasizing the methods. Providing enough flexibility to test different robot architectures and manufacturing processes. As an example, two robot prototypes are shown.

Kang et al. [30] developed a dynamic modelling and control of continuum arm robot for a multiple continuum arm inspired by live octopuses. The kinematics and dynamics

for a single arm are analyzed including the longitudinal muscles, radial muscles, isovolumetric constraints, and interaction between an object. The interaction behavior between the arm and the surrounding environment are taken into account for hydrodynamic forces and suckers. Simulation results show that the obtained model is capable of producing highly dexterous single and multiple arm motions that are similar to live Octopus movements.

1.6 Objectives

The objectives of the present work are given as follows.

- To create a robotic arm that can be fixed on the roof in industries.
- To understand the geometry and applications of industrial robot manipulator.
- To study the motion simulation of a real-time prototype and generate a required path function for robotic arm.
- To study the behavior of the proposed robotic arm using static and dynamic analysis.

1.7 Work Contributions

- In this project, the study of various robotic arm configuration has been carried out and have chosen a robotic manipulator to fulfill our requirement.
- A robotic arm is designed using CAD and Dynamic simulations.
- ANSYS workbench is used to identify the structural analysis and transient analysis of the robotic arm.
- A forward kinematic analysis of a robotic arm is carried out using computer program.

2 Modelling of a Robotic Arm

2.1 Assumptions

- An industrial robotic arm is taken as reference and the scale of the industrial robotic arm is reduced to 1/5th of its original measurements.
- Generally, most of the industrial robotic arms are mounted on the floor or on the side of the wall. But we are fixing the robotic arm on the roof of the workshop.
- The model of robotic arm consists of 6 links considered from a reference model in which there are 1-linear joint and 5-revolute joints.
- The linear joint is fixed at one end to the roof and the other end is having a prismatic link.
- The material considered for the robotic arm is stainless-steel.

2.2 Design of a 6-DOF robotic arm

The arc welding robotic arm is designed using CATIA software, dimensions of each link is mentioned in the shown in Fig. 2.1. The arc welding robotic arm and all the links and joints are named according to their respective positions.

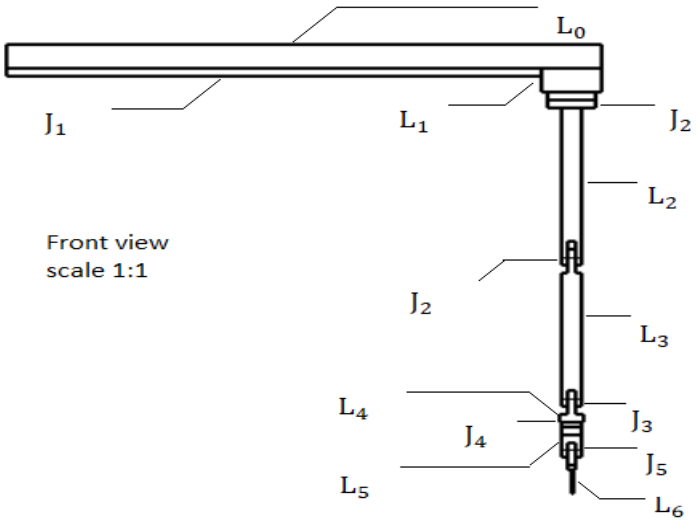

Figure 2-1 Model of arc welding robotic arm

L_0 is represents first link, L_1 represents second link, J_1 represents first joint and vice versa. There are 6 different parts in the robotic arm shown which are drawn as part drawings in CATIA and are assembled together. Link-1 in the assembly is designed by

drawing its layout and then using pad command the part is extruded. Link-1 is having a linear joint which is drawn by giving grooves in the model. Link-2 and other parts are modeled in the similar fashion and all the parts are saved for assembly. The assembly of all the parts is done using assembly tool and assembled by coinciding each part with its axis.

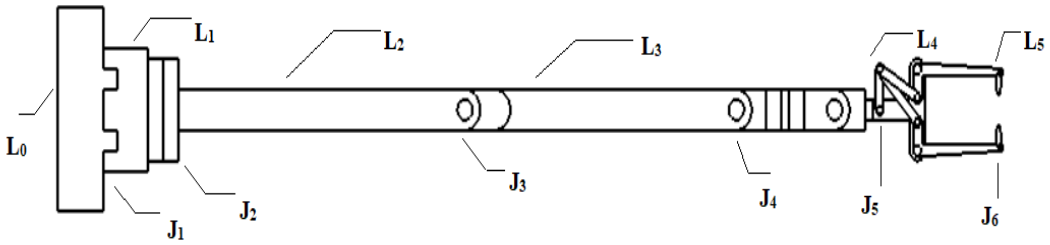

Figure 2-2 Model of Spot-welding robotic arm

The Fig. 2.2 shows the model of spot-welding robotic arm designed in a similar way of arc welding robotic arm in Fig. 2.1. The design of gripper for spot-welding robotic arm is shown in the Fig. 2.4, which has 2-DOF for spot welding. The robotic arm is considered with a steel and the material properties and geometric parameters are given in Tables 2.1 and 2.2 respectively.

Table 2-1 Material properties of a robotic arm

Properties	Values
Young's Modulus	$2x10^{11}$ Pa
Poisson's Ratio	0.3
Bulk Modulus	$1.667x10^{11}$ Pa
Shear Modulus	$7.692x10^{10}$ Pa
Density	7850 kgm^{-3}

Table 2-2 Geometrical parameters of a robotic arm

Link	Length (mm)	Width/radius (mm)	Thickness (mm)
L_1	600	100	30
L_2	40	25	10
L_3	200	20	20
L_4	180	20	20
L_5	35	35	10
L_6	30	40	20

2.3 Joint movements

Model of the robotic arm is designed in CATIA which is exported as step file to ADAMS software for assigning joint movements like linear and revolute joints. In the robotic arm there are 5-revolute joints and 1-linear joint. So, the linear and revolute joints are shown in Fig. 2.3. Joints and Motions are given to each link using ADAMS. The simulation for joints and motions of each link is checked using simulation tool. The simulation of joints is given using step functions for each joint in which the motion of the links is varied according to the time allotted.

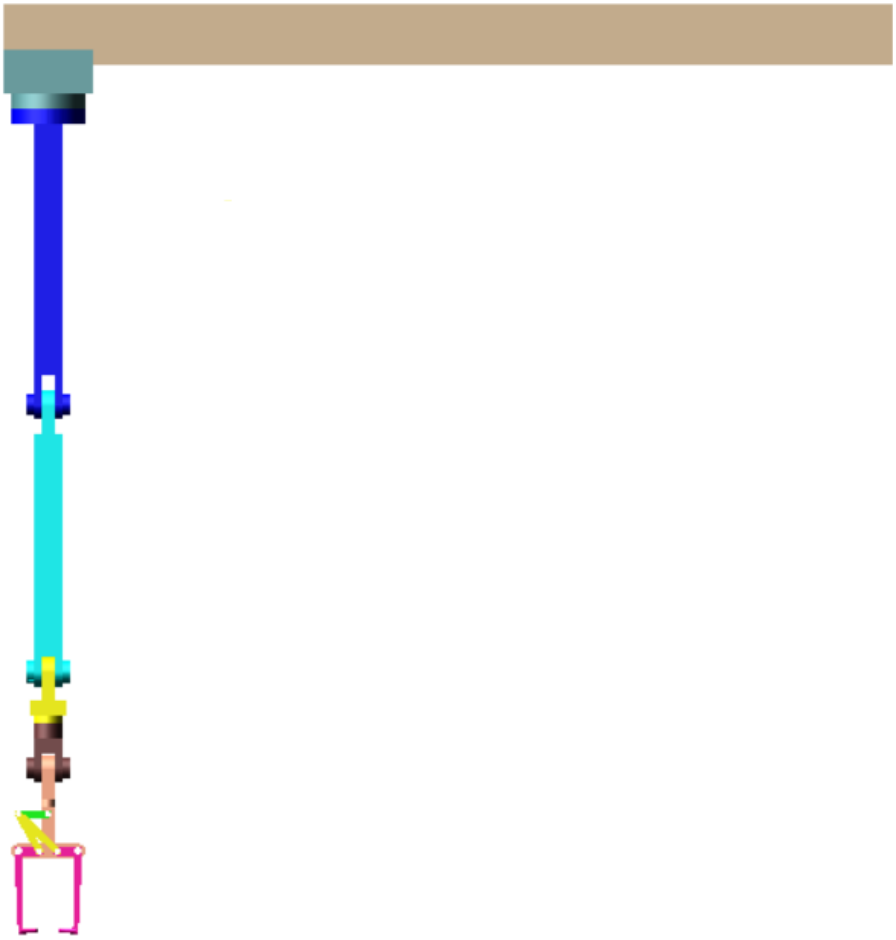

Figure 2-3 Robotic arm for Spot welding using ADAMS

- The Fig. 2.3 is the robotic arm modeled in CATIA and joint movements were given in ADAMS which is having a 6-DOF with a spot-welding gripper at the end-effector.

2.4 Modeling of a Gripper

Gripper for robotic arm which is at the end of the robotic arm, so it is called end-effector of the robotic arm. Modelling of gripper is done using CATIA which is having a revolute and prismatic links. The gripper is used for spot welding, so it is having two electrodes which have linear joint and a revolute joint, the joint movements were given using ADAMS. Two types of grippers are modeled for spot welding and arc welding which have two degrees of freedom i.e., one revolute and one prismatic are shown in Fig. 2-4.

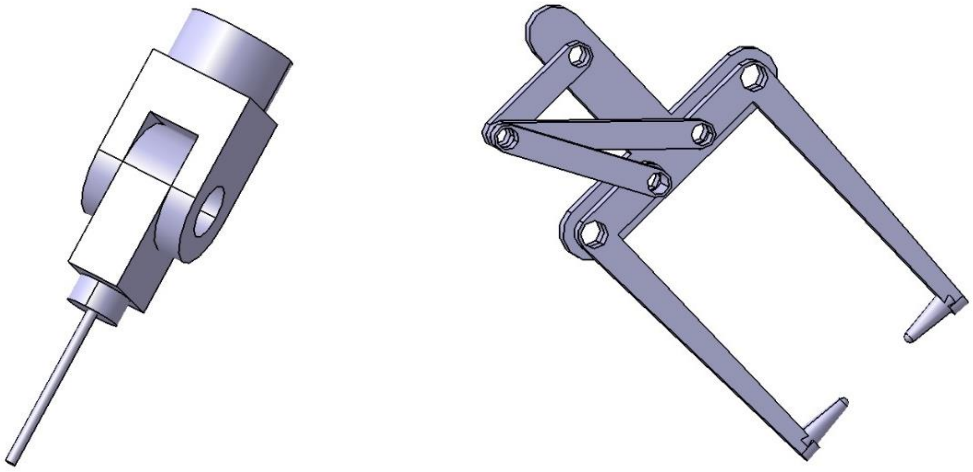

(a) Arc welding gripper (b) Spot-welding gripper

Figure 2-4 Grippers for arc welding and spot-welding

2.5 Welded joints for arc welding

The basic welded joints like V-butt, lap and T-joint are considered for the simulation of robotic arm are shown in Fig. 2-5.

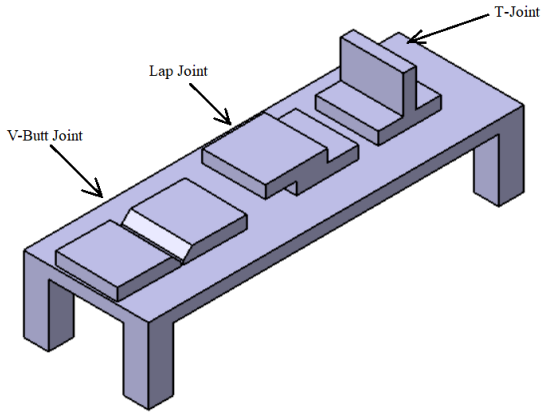

Figure 2-5 Workbench with different types of joints for arc welding

A **welding joint** is a point or edge where two or more pieces of metal or plastic are joined together. They are formed by welding two or more workpieces (metal or plastic) according to a particular geometry. There are five types of joints referred to by the American Welding Society: butt, corner, edge, lap, and tee. These configurations may have various configurations at the joint where actual welding can occur.

There are many types of butt welds, but all fall within one of these categories: single welded butt joints, double welded butt joint, and open or closed butt joints. A single welded butt joint is the name for a joint that has only been welded from one side. A double welded butt joint is created when the weld has been welded from both sides. With double welding, the depths of each weld can vary slightly. A closed weld is a type of joint in which the two pieces that will be joined are touching during the welding process. An open weld is the joint type where the two pieces have a small gap in between them during the welding process.

The Tee Weld Joint is formed when two bars or sheets are joined perpendicular to each other in the form of a T shape. This weld is made from the resistance butt welding process. It can also be performed by Extrusion Welding. Usually two flat pieces of poly are welded at 90 degrees to each other, and extrusion welded on both sides.

Thin sheet metals are often flanged to produce edge-flange or corner-flange welds. These welds are typically made without the addition of filler metal because the flange melts and provides all the filler needed. Pipes and tubing can be made from rolling and welding together strips, sheets, or plates of material.

Flare-groove joints are used for welding metals that, because of their shape, form a convenient groove for welding, such as a pipe against a flat surface.

3 Kinematic Analysis of a 6-DOF robotic arm

3.1 Kinematic Analysis

A serial manipulator consists of a fixed base, a series of links connected by joints, and ending at a free end carrying the tool or the end-effector. In contrast to parallel manipulators, there are no closed loops. By actuating the joints, one can position and orient the end-effector in a plane or in three-dimensional space to perform desired tasks with the end-effector. The serial manipulator geometries are described using the well-known Denavit-Hartenberg (D-H) parameters. There are two important aspects in kinematic analysis of robots, the Forward Kinematics problem and the Inverse Kinematics problem. Forward kinematics refers to the use of the kinematic equations of a robot to compute the position of the end-effector from specified values for the joint parameters Inverse kinematics refers to the use of the kinematics equations of a robot to determine the joint parameters that provide a desired position of the end-effector.

A serial-link manipulator consists of a set of bodies, called links, in a series and connected by joints. A link is considered a rigid body that defines the spatial relationship between two neighboring joint axes. The objective of forward kinematic analysis is to determine the cumulative effect of the entire set of joint variables.

3.2 Kinematic relation between adjacent links

To find the transformation matrix between two frames which are adjacent to each other, consider frame $\{i-1\}$ and $\{i\}$ as shown in the Fig. 3.1. The kinematic joint link parameters involved $(\theta_i,\ d_i, a_i, \alpha_i)$. The general transformation of frame from $\{i-1\}$ and $\{i\}$ consists of displacement of co-ordinate system and rotation of a particular axes.

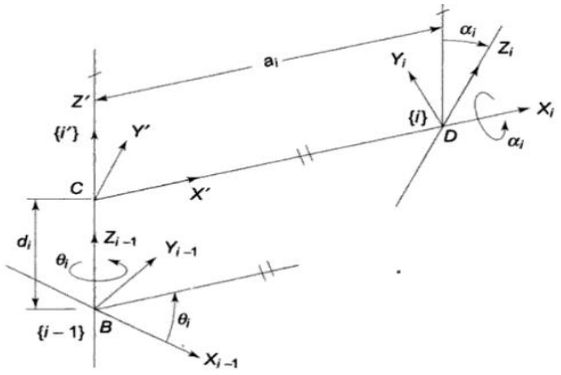

Figure 3-1 Kinematic relation between two links

3.3 Forward Kinematic analysis of a 6-DOF

The forward kinematic equations can be calculated for any given type of robotic manipulators depending on the relationship among the position, the orientation of the articulated arm end effector and the other individual joints. The variables for rotational joints are the angles between the links that connected the joints, should be specified like for the first link the variable is L_0, for second link L_1 and vice-versa. The joint variables are given like for first joint it is j_1, second joint is j_2 and vice-versa.

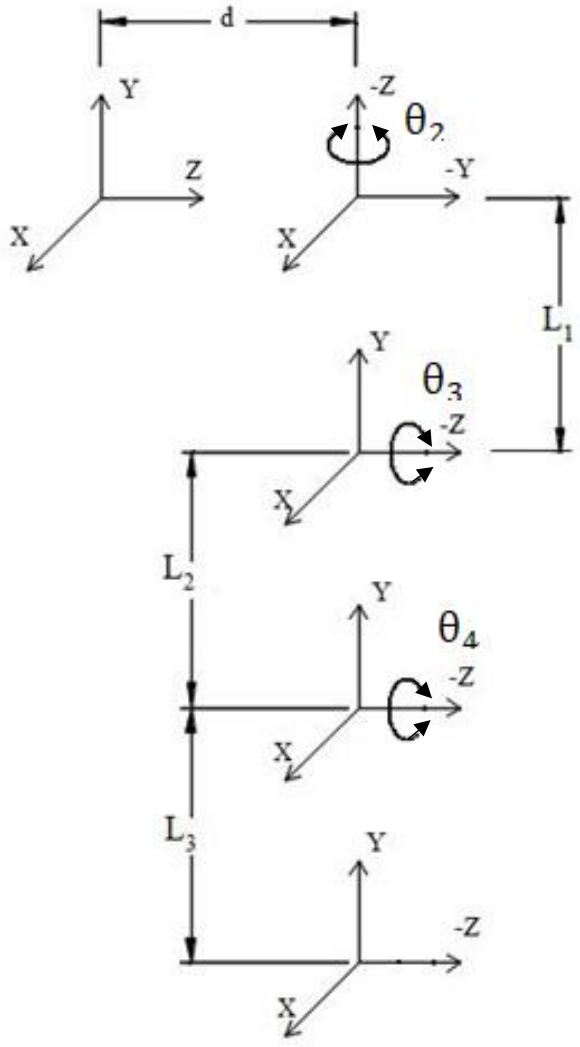

Figure 3-2 Representation of frames

With the help of D-H notations, $\{i-1\}$ and $\{i\}$ frames are shown according to the represented angles of links and link displacements are shown in Fig. 3-2.

Table 3-1 D-H notation for the modelled robotic arm

S.NO	L_i	α_i	d_i	θ_i	cos θ	sin θ	cos α	sin α
1	L_1	0	d_1	0	1	0	1	0
2	L_2	-90	0	θ_2	$\cos\theta_2$	$\sin\theta_2$	0	-1
3	L_3	90	0	θ_3	$\cos\theta_3$	$\sin\theta_3$	0	1
4	L_4	0	0	θ_4	$\cos\theta_4$	$\sin\theta_4$	1	0

The Table 3.1 represents the D-H notation of the robotic arm which is used for forward analysis of manipulator. The parameters like L_i represents length of the robotic arm link, α_i represents the angular displacement of the axis of the link, d_i represents the linear displacement of the links, θ_i represents the angle between links.

$$ {}^{0}\mathbf{T}_{1}\,(\boldsymbol{\theta_1}) = \begin{bmatrix} 1 & 0 & 0 & L_1 \\ 0 & 1 & 0 & 0 \\ 0 & 0 & 1 & d_1 \\ 0 & 0 & 0 & 1 \end{bmatrix} \tag{3.1} $$

$$ {}^{1}\mathbf{T}_{2}\,(\boldsymbol{\theta_2}) = \begin{bmatrix} C\theta_2 & 0 & -S\theta_2 & L_2C\theta_2 \\ S\theta_2 & 0 & C\theta_2 & L_2S\theta_2 \\ 0 & -1 & 0 & d_1 \\ 0 & 0 & 0 & 1 \end{bmatrix} \tag{3.2} $$

$$ {}^{2}\mathbf{T}_{3}\,(\boldsymbol{\theta_3}) = \begin{bmatrix} C\theta_3 & 0 & S\theta_3 & L_3C\theta_3 \\ S\theta_3 & 0 & -C\theta_3 & L_3S\theta_3 \\ 0 & 1 & 0 & 0 \\ 0 & 0 & 0 & 1 \end{bmatrix} \tag{3.3} $$

$$ {}^{3}\mathbf{T}_4(\boldsymbol{\theta_4}) = \begin{bmatrix} C\theta_4 & -S\theta_4 & 0 & L_4C\theta_4 \\ S\theta_4 & C\theta_4 & 0 & L_4S\theta_4 \\ 0 & 0 & 1 & 0 \\ 0 & 0 & 0 & 1 \end{bmatrix} \tag{3.4} $$

The assembly of individual transformation matrix for the forward kinematic analysis is given in the Eq. 3.5. ${}^{0}\mathbf{T}_4 = {}^{0}\mathbf{T}_1\ {}^{1}\mathbf{T}_2\ {}^{2}\mathbf{T}_3\ {}^{3}\mathbf{T}_4 =$

$$ \begin{bmatrix} C\theta_2C\theta_3C\theta_4 - S\theta_2S\theta_4 & -C\theta_2C\theta_3S\theta_4 - S\theta_2C\theta_4 & C\theta_2S\theta_3 & L_4C\theta_2C\theta_3C\theta_4 - L_4S\theta_2S\theta_4 + L_3C\theta_2C\theta_3 + L_2C\theta_2 + L_1 \\ S\theta_2C\theta_3\cos\theta_4 + C\theta_2S\theta_4 & -S\theta_2C\theta_3S\theta_4 + C\theta_2C\theta_4 & S\theta_2S\theta_3 & L_4S\theta_2C\theta_3C\theta_4 + L_4C\theta_2S\theta_4 + L_3S\theta_2C\theta_3 + L_2S\theta_2 \\ -S\theta_3C\theta_4 & S\theta_3S\theta_4 & C\theta_3 & -L_4S\theta_3C\theta_4 - L_3S\theta_3 + d_1 \\ 0 & 0 & 0 & 1 \end{bmatrix} \tag{3.5} $$

From the Eq. (3.5), the end-effector co-ordinates which are used to find workspace of the robotic arm.

3.4 Workspace Analysis

Using the forward kinematic analysis, a reachable work-volume and proposed 6-DOF arm is shown in Fig. 3.3. This analysis of the manipulator is done to know the co-ordinates of the robotic arm that can be covered.

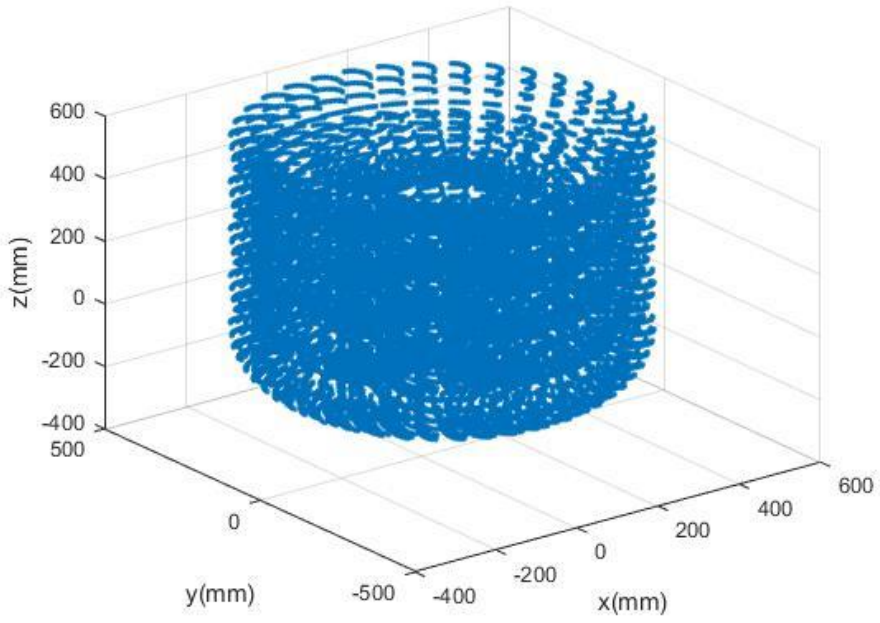

Figure 3-3 Workspace analysis of the robotic arm

MATLAB program is developed with the help of D-H notations from forward kinematic analysis. D-H notation is solved with the joint link parameters from which transformation matrix is obtained, from the transformation matrix we can get the positions of the end-effector by changing the link angles from 0 to 360˚. The data collected from the transformation matrix gives the workspace of the robotic arm in MATLAB. The workspace in 3D generated is shown in Fig. 3-3, the maximum limits in x-direction is -400 to 600 mm. Similarly, maximum limits along y and z axes are (-500 to 500 mm), (-400 to 600 mm). Based on the link lengths and work space generated in MATLAB the approximate work volume is 0.5026 m^3

3.5 Simulation of arc welding

After assigning all the joints and motions of the arc welding robotic arm, for the simulation of arm step functions are given which makes the joints to move the links at particular time with that particular displacement and degrees of rotation. The syntax for step functions is STEP (time, initial time, initial angle, final time, final angle), e.g.: STEP (time, 0, 0, 5.0, 60d).

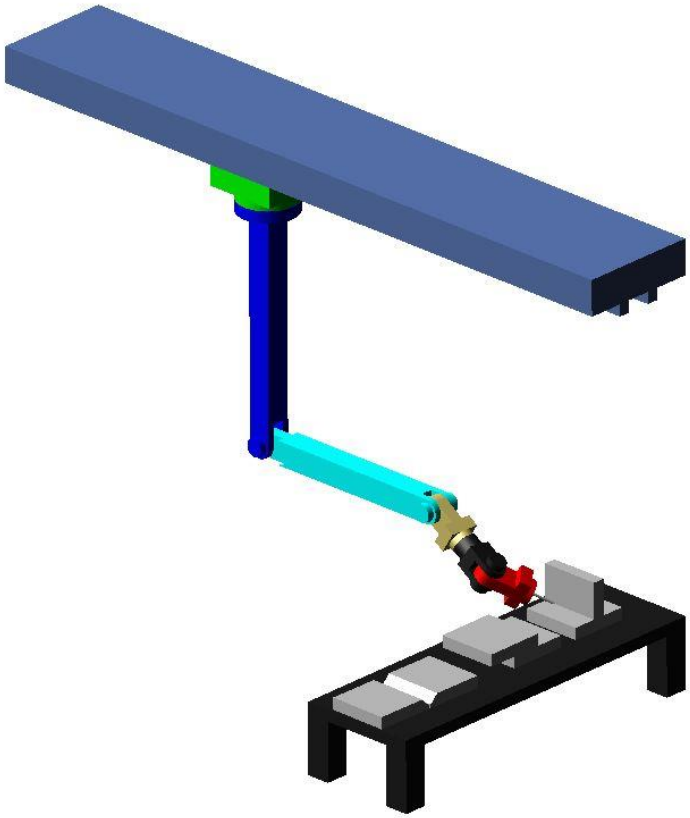

Figure 3-4 Simulation of arc welding for various joints

Table 3-2 Step functions for arc welding robotic arm

Time (sec)	**Type of Joint**	0.0	5.0	10.0	15.0	20.0	30.0
Joint-1	Linear (m)	0.0	0.17	0.06	0.12	0.08	-0.27
Joint-2	Revolute (degrees)	-	-3.0	-	-	-	-30
Joint-3	Revolute (degrees)	-	-	-87	15	-	-30
Joint-4	Revolute (degrees)	-	-	-	-	-35	20
Joint-5	Revolute (degrees)	-	17	-17	-45	90	-
Joint-6	Revolute (degrees)	-	0.0	90.0	90	-	-100

The Table 3-2 represents the step functions for arc welding robotic arm for making arc welding at required places. The simulation for general arc welded joints is shown in the Fig. 3-4.

3.6 Simulation of spot-welding

The simulation of the spot-welding robotic arm is as similar as the simulation of arc welding robotic arm except a change in the time step functions which is represented in the following Table 3-3.

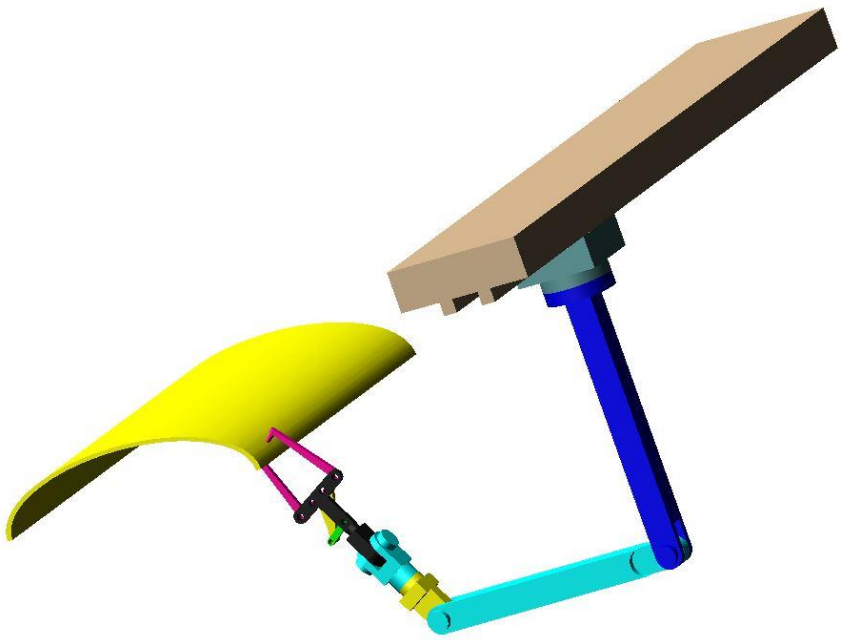

Figure 3-5 Simulation for spot welding on a sheet metal

Table 3-3 Step functions for spot-welding robotic arm

Time (sec)	**Type of Joint**	0.0	3.0	6.0	9.0	12.0	15.0
Joint-1	Linear (m)	0.0	0.54	-0.15	-0.09	-0.09	-0.1
Joint-2	Revolute (degrees)	0.0	0.0	0.0	0.0	0.0	0.0
Joint-3	Revolute (degrees)	0.0	-90	0.0	0.0	0.0	90
Joint-4	Revolute (degrees)	0.0	60	0.0	0.0	0.0	0.0
Joint-5	Revolute (degrees)	0.0	0.0	-90	0.0	0.0	0.0
Joint-6	Torque (N-m)	0.0	0.0	0.4	0.0	0.0	-0.4

The simulation for spot welding on a sheet metal is shown in Fig. 3-5. The Table 3-3, represents step functions for spot-welding robotic arm which has different time step functions compared to arc welding robotic arm and this robotic arm requires continuous straight-line motion which is given in the step functions.

Torque for end-effector in spot welding which are given is shown in Fig. 3-3 Average torque applied on the gripper for spot welding is 0.4 N-m. Spot welding at (5-6) sec., (9-10) sec. and (11-13) sec. is applied.

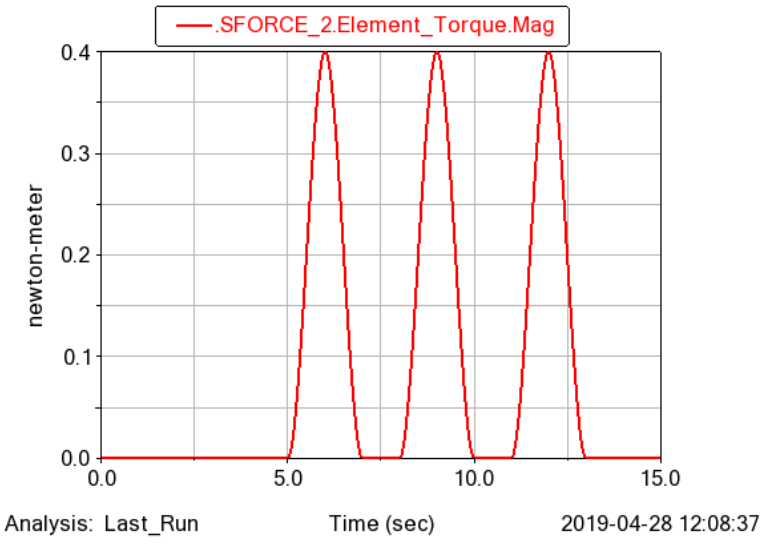

Figure 3-6 Torque at links for motion

3.7 Results and Discussion

3.7.1 Joint displacements of a 6-DOF

- Joint displacements generated due to step functions is shown in the Fig. 2.3.

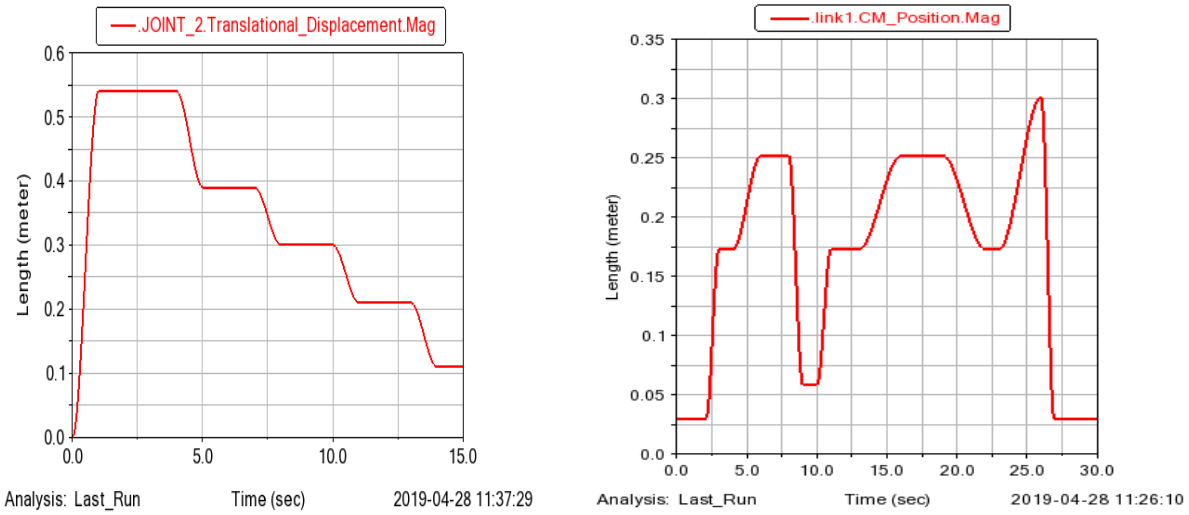

(a) Spot welding (b) Arc welding

Figure 3-7 Graph b/w Length vs Time for spot welding and arc welding simulation

In the Fig 3.7, a graph between length vs time is shown when the simulation of robotic arm using spot welding gripper and the horizontal lines represent the welding process of the robotic arm.

3.7.2 Contact forces for Spot welding

In spot welding, there are two electrodes which are used to generate spot welds when a required amount of force is applied. To apply spot weld between two materials there must be some force between electrodes, that force is called contact force. When 0.4 N-m is applied on the gripper 0.75 N force is generated on the workpiece.

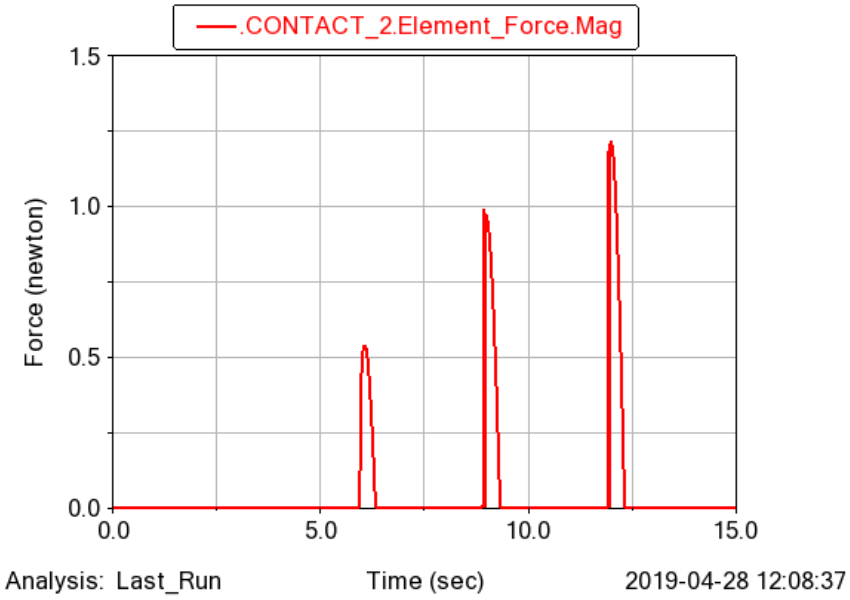

Figure 3-8 Contact forces for spot welding

There are three peaks in the Fig. 3.8, which represents three contact forces of the electrodes at three different time periods.

3.7.3 Electrode displacement in arc welding

During arc welding, the electrode at the gripper melts to make a weld bead, so the movement of the electrode is important in the simulation of the arc welding robotic arm. The electrode displacement of the arc welding gripper is shown in the Fig. 3.9 as the time increases, the displacement at end point of the electrode increases at zones 1,2 and 4 due to forward motion and at zone 3 it decreases due to backward motion as seen in the graph.

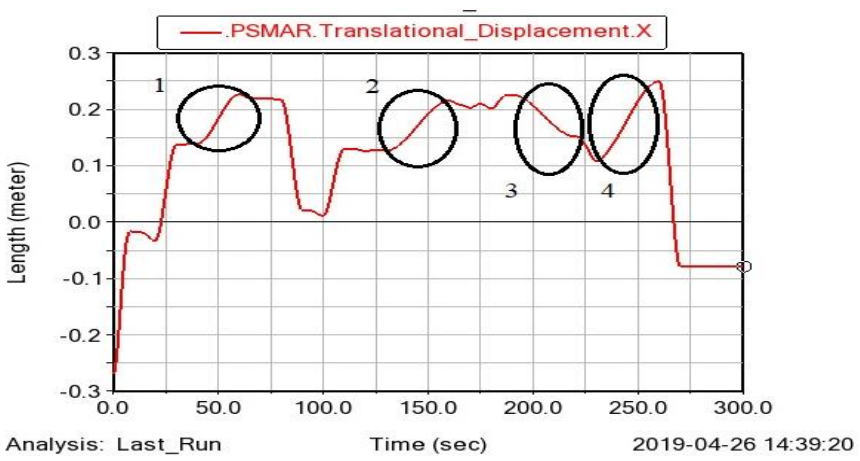

Figure 3-9 Electrode displacement in arc welding

Results and discussion

- In the simulation of robotic arm for arc welding and spot welding, the joint displacements, torque of the manipulator are shown in Fig 3.6, 3.7 respectively.
- The maximum torque given to simulate the robotic arm is 0.4 N-m and the maximum displacement of robotic arm for arc welding is 0.35 m.
- Maximum electrode displacement for arc welding robotic arm is 0.59 m.
- The maximum displacement of robotic arm for spot-welding is 0.55 m and maximum contact forces between each electrode is 0.85 N.
- With all these loads applied on the robotic arm, the manipulator is still not deformed and the structure can withstand loads that are even higher than these loads.

4 Structural analysis of a 6-DOF robotic arm

4.1 Static structural analysis

Structural analysis is the determination of the effects of loads on physical structures and their components. Structures subject to this type of analysis include all that must withstand loads, such as buildings, bridges, vehicles, furniture, attire, soil strata, prostheses and biological tissue. Steady loading is assumed that it changes with change in time and vary slowly. Static structural analysis can be done using ANSYS workbench.

A static structural analysis can be either linear or nonlinear. All types of nonlinearities are allowed - large deformations, plasticity, stress stiffening, contact elements, hyper elasticity and so on. Structural analysis is done for every structure to analyse its structural strength that it can with-stand the static loading without any deformation. There are two types of loads that can be applied for static structural analysis, first is dead loads which are the original weight of the structure which are permanently attached to the structure without applying any external loads. Second is the kind of loads which are acting on the structure externally which vary according to time and magnitude, like impact loads, earthquake loads, wind loads, etc.,

To perform an accurate analysis a structural engineer must determine information such as structural loads, geometry, support conditions, and material properties. There are three approaches to the analysis: the strength of materials approach, the continuum mechanics approach and the finite element approach. The finite element method is numerical method analysis for solving differential equations generated by continuum mechanics and strength of materials.

The robotic manipulator which is designed using CATIA is analysed using ANSYS workbench about its static analysis. First the assembly body from CATIA is imported through step file format and mentioned its geometry and material properties. Then, by meshing the entire model using finite element method and after that one link is fixed and a force is given to the manipulator to know its static analysis.

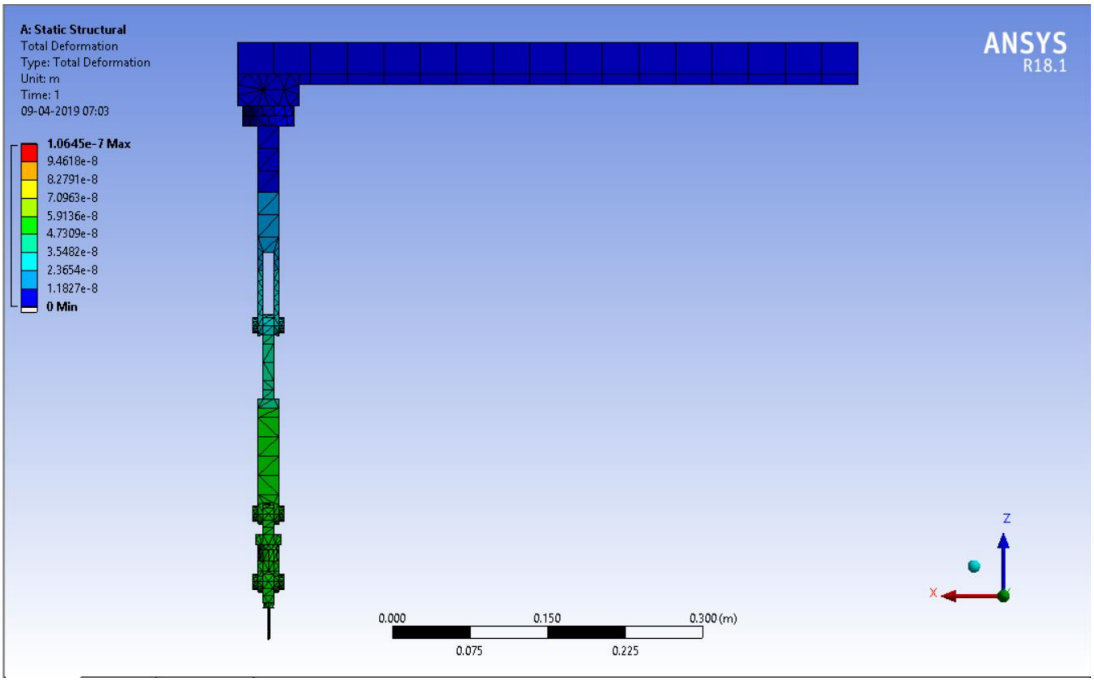

Figure 4-1 Static analysis of arc welding robotic arm

The Fig. 4-1 shows the static structural analysis of an arc welding robotic arm.

4.1.1 Results and discussion

- Structural analysis is the analysis of a body which can withstand its structure when various loads are applied on the body.
- There are various types of structural analysis in which two types were used to analyze the robotic arm. They are Static structural analysis and Transient structural analysis.
- In static structural analysis, the analysis of the body weight is tested i.e., whether the robotic arm can bear its own weight. Maximum total deformation in the robotic arm is 1.064e-7 which is very low because the robotic arm can bear its body weight.

Table 4-1 Maximum and minimum values of Total deformation

Total Deformation	Value (m)
Minimum deformation	0
Maximum deformation	1.064e-7

4.2 Transient Structural Analysis

Transient structural analysis is the analysis done when the loads changes with time and this analysis uses Mechanical APDL solver to solve. Transient analysis can also be done for flexible as well as rigid bodies. This type of analysis used to identify the dynamic response of the structure by action of displacement loads. A transient structural analysis can be either linear or nonlinear. All types of nonlinearities are allowed - large deformations, plasticity, contact, hyper elasticity, and so on. ANSYS Workbench offers an additional solution method of Mode-Superposition to perform linear transient structural analysis.

- In transient analysis, joint loads are given according to their respective joint type using time step functions.
- For prismatic link, time steps given in displacement for a particular time and at the remaining time it becomes constant.
- For revolute joint, time step functions are given in degrees and vice versa.

Deformation in continuum mechanics is the transformation of a body from a reference configuration to a current configuration. A configuration is a set containing the positions of all particles of the body.

A deformation may be caused by external loads, body forces, changes in temperature, moisture content, or chemical reactions, etc. Strain is a description of deformation in terms of relative displacement of particles in the body that excludes rigid-body motions. Different equivalent choices may be made for the expression of a strain field depending on whether it is defined with respect to the initial or the final configuration of the body and on whether the metric tensor or its dual is considered.

Table 4-2 Total deformation in Transient analysis

Total Deformation	Value
Minimum Deformation	4.36e-19
Maximum Deformation	0.319

- In transient structural analysis, the total deformation of the robotic arm is shown in 360 seconds of time step functions, as shown in the Table 4-2.
- The time step functions for each joint is given with a time interval of 60 seconds, which given a total 360 seconds of time step functions.

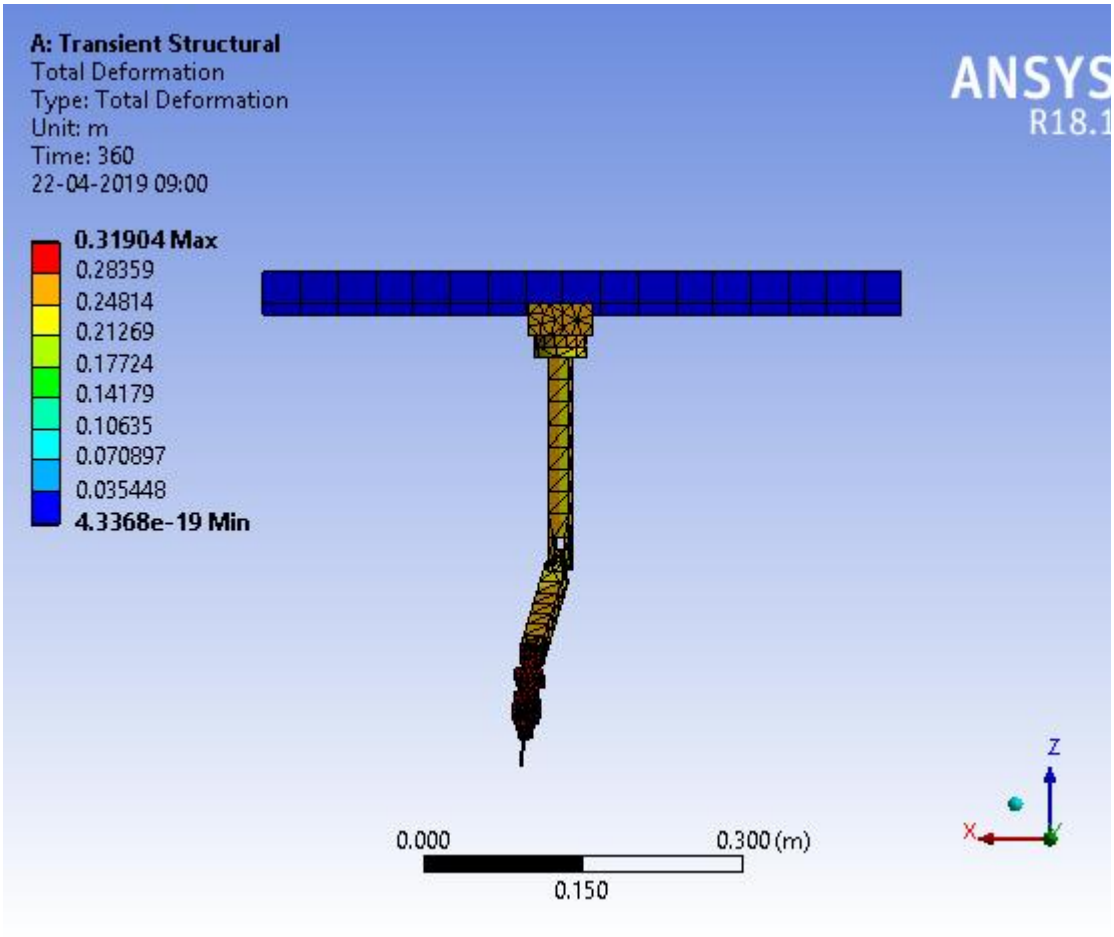

Figure 4-2 Transient analysis of arc welding robotic arm

In the Fig. 4-2, transient analysis of total deformation is shown and the maximum and minimum deformation values are shown in the Table 4.2.

Results and discussion

In Transient structural analysis, various loads are applied on the robotic arm at variable time and load values using time step functions. The maximum total deformation of the robotic arm is 0.319 as shown in the Table 4-2.

Equivalent von-mises stress

Equivalent stress also called von Mises stress is often used in design work because it allows any arbitrary three-dimensional stress state to be represented as a single positive stress value. Equivalent stress is part of the maximum equivalent stress failure theory used to predict yielding in a ductile material. The von Mises stress is used to predict yielding of materials under complex loading from the results of uniaxial tensile tests. The von Mises stress satisfies the property where two stress states with equal distortion energy have an equal von Mises stress.

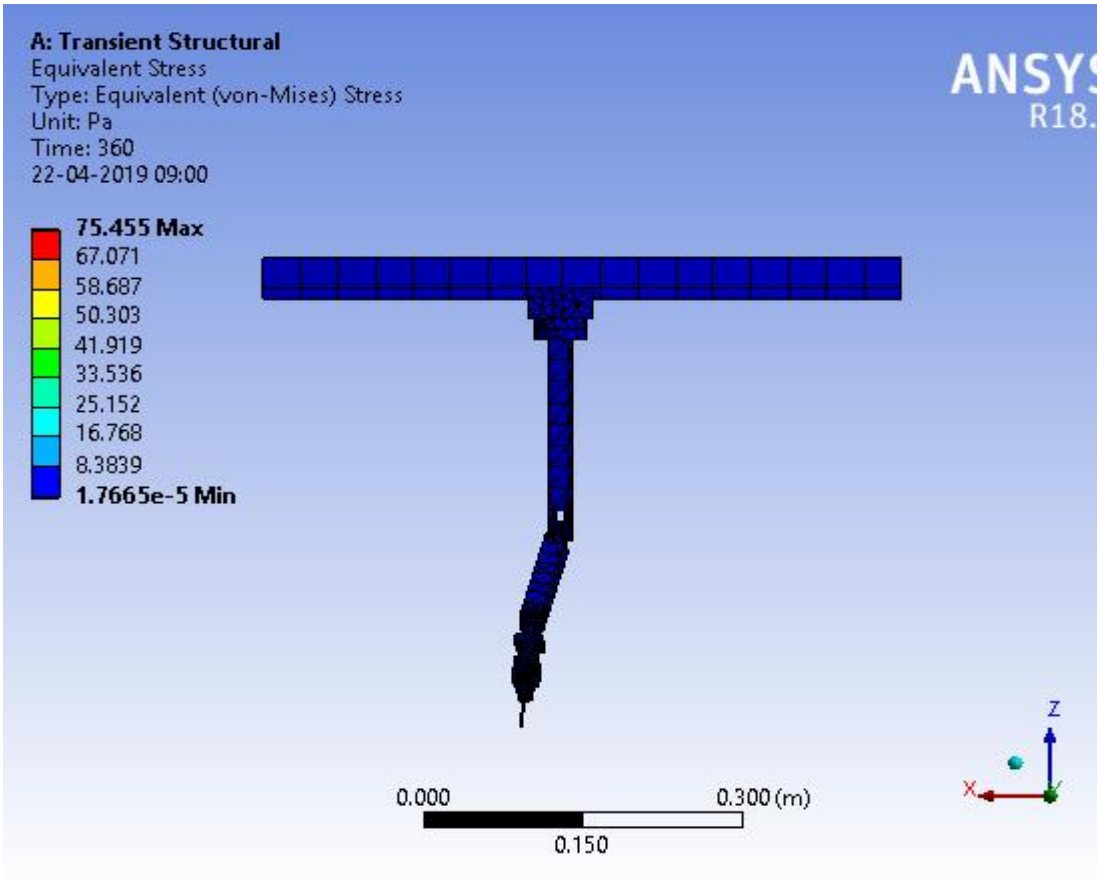

Figure 4-3 Equivalent von-mises stress analysis

The Fig. 4-3 shows the Equivalent von-Mises stress of the robotic arm and the maximum-minimum values are shown in the Table 4-3.

Results and discussion

The maximum stress developed during equivalent von-mises stress is 75.455 Pa and the minimum stress developed is 1.77e-5 Pa. The red colour shown in the Fig. 4-3

experiences maximum stress and at blue colour region represents minimum stress acting on the robotic arm.

Table 4-3 Maximum and minimum values of Equivalent von-mises stress analysis

Equivalent stress	Value (Pa)
Minimum stress	1.7667e-5
Maximum stress	75.455

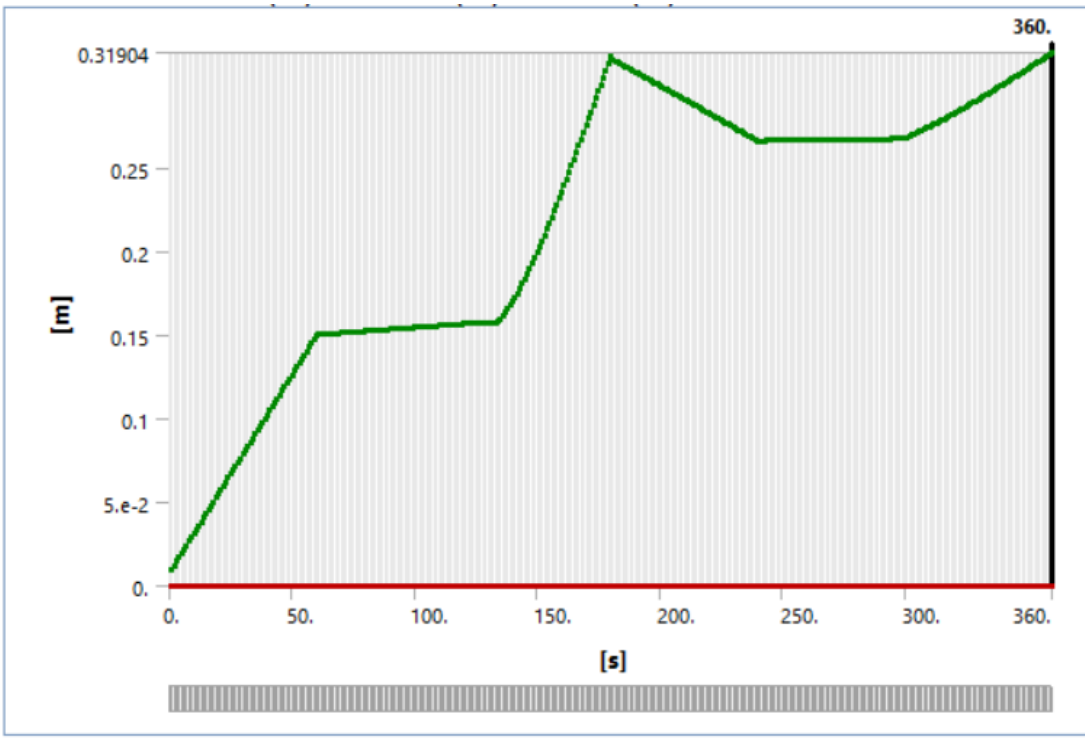

Figure 4-4 Graph between distance vs time in Time step functions

A graph is plotted between distance and time which shows the time step functions up to 360 seconds as shown in the Fig. 4-4.

4.3 Modal analysis

Modal analysis is the study of the dynamic properties of systems in the frequency domain. Examples would include measuring the vibration of a car's body when it is attached to a vibrator, or the noise pattern in a room when excited by a loudspeaker. Modern day experimental modal analysis systems are composed of sensors such

as transducers, or non-contact via a Laser vibrometer, data acquisition system and an analogy-to-digital converter front end and host PC, to view the data and analyse it.

In structural engineering, modal analysis uses the overall mass and stiffness of a structure to find the various periods at which it will naturally resonate. These periods of vibration are very important to note in earthquake engineering, as it is imperative that a building's natural frequency does not match the frequency of expected earthquakes in the region in which the building is to be constructed. If a structure's natural frequency matches an earthquake's frequency, the structure may continue to resonate and experience structural damage. Modal analysis is also important in structures such as bridges where the engineer should attempt to keep the natural frequencies away from the frequencies of people walking on the bridge.

Vibration analysis of industrial machinery has been around for many decades, but gained prominence with the introduction and widespread use of the personal computer. Vibration Analysis refers to the process of measuring the vibration levels and frequencies of industrial machinery, and using that information to determine the "health" of the machine, and its components.

When an industrial machine (such as a fan or pump) is operated, it generates vibration. This vibration can be measured, using a device called an accelerometer. An accelerometer generates a voltage signal, proportional to the amount of vibration, as well as the frequency of vibration, or how many time per second or minutes the vibration takes place. This voltage signal from the accelerometer is fed into a data collector, which records this signal as either a time waveform (amplitude vs. time), as a Fast Fourier Transform (amplitude vs. frequency), or as both. This signal can then be analysed by a trained vibration analyst, or by the use of a "smart" computer program algorithm. The analysed data is then used to determine the "health" of the machine, and identify any impending problems in the machine, such as misalignment, unbalance, a bearing or lubrication problem, looseness, and more.

The use of vibration analysis can determine problems caused due to improper installation, machining errors, insufficient lubrication, improper shaft or sheave alignment, loose bolting, bent shafts, and much more. It can, in most cases, detect these problems long before the damage can be seen by maintenance, and long before it damages other machine components.

The use of vibration analysis, condition monitoring, or predictive maintenance has made great strides increasing the usable life of machinery.

Modal analysis gives you the information regarding the different modes of vibration i.e., different shape that can be taken up by the structure during vibration. This shape during different modes are called mode shape and all mode shapes have their corresponding natural frequency. Modes are inherent properties of a structure, and are determined by the material properties like mass, damping, and stiffness, and boundary conditions of the structure. Each mode is defined by a natural frequency, modal damping, and a mode shape i.e. the so-called "modal parameters". If either the material properties or the boundary conditions of a structure change, its modes will change. For instance, if mass is added to a structure, it will vibrate differently. Natural frequency is the frequency with which the structure vibrates when an external vibrating source is present like when soldiers are required to break their steps which created vibrations on the bridge. To understand this, we will make use of the concept of single and multiple-degree-of-freedom systems. Mode shapes are given like Mode-1, Mode-2, and so-on which are the vibrations created at various different links which have different DOF.

For the robotic manipulator, we used 6 modes because the manipulator is having 6 DOF. The following is the table which has 6 modes and their relevant frequency acting on the robotic arm.

4.4 Modal analysis

Modal analysis is used to determine natural frequency of a body when various loads are acting on the body. According to the number of links, the number of mode shapes varies. For this mechanism a 6 different mode shapes are obtained in which the first three mode shapes are shown in the Fig. 4-5 in which various frequencies are acting at different directions on the robotic arm.

Results and discussion

For mode-1 and 2 there is a slight change in the frequency of vibration as shown in Fig. 4-5, i.e., 85.816 and 89.67 Hz. At mode-3 there is a sudden change in the vibrations due to more number of joints in the robotic arm.

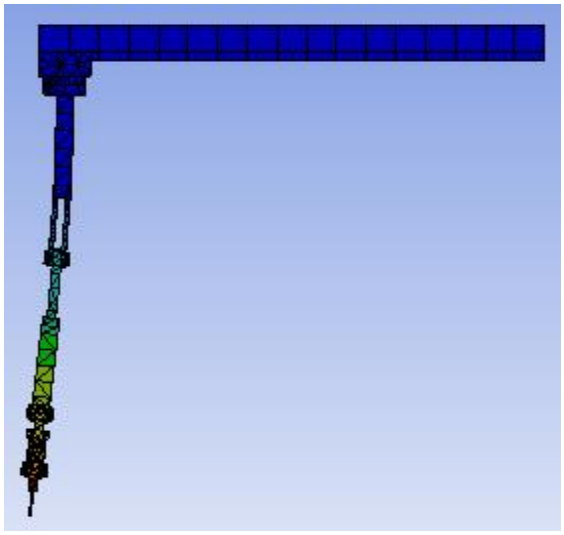

Mode-1(a)
(85.816 Hz)

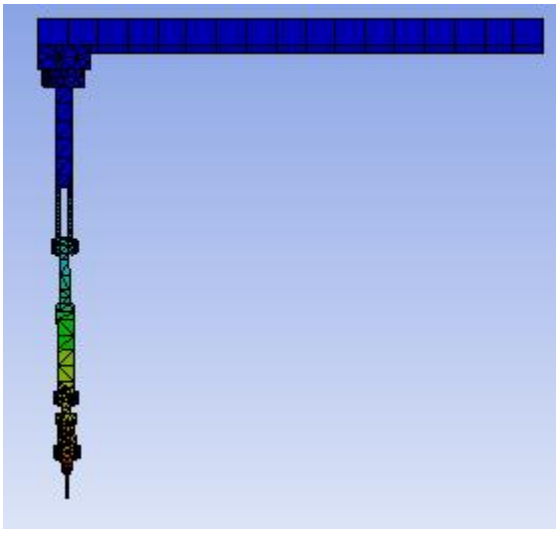

Mode-2 (b)
(89.67 Hz)

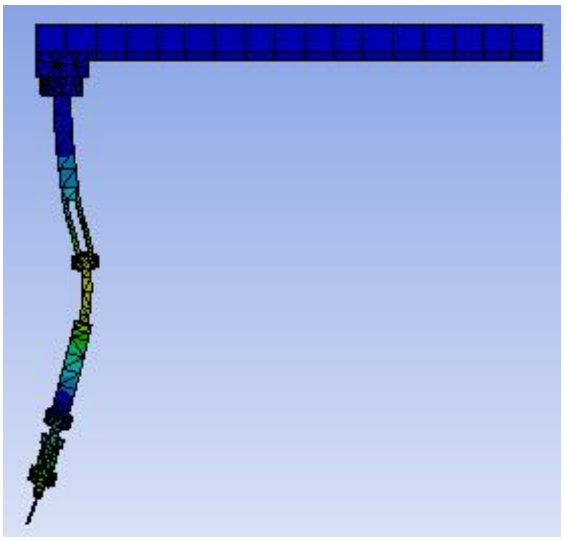

Mode-3 (c)
(378.25 Hz)

Figure 4-5 Types of modes in Modal analysis

4.5 Results and Discussion

- Structural analysis is the analysis of a body which can withstand its structure when various loads are applied on the body.

- There are various types of structural analysis in which two types were used to analyze the robotic arm. They are Static structural analysis and Transient structural analysis.
- In static structural analysis, the analysis of the body weight is tested i.e., whether the robotic arm can bear its own weight. Maximum total deformation in the robotic arm is 1.064e-7 which is very low because the robotic arm can bear its body weight.
- In Transient structural analysis, various loads are applied on the robotic arm at variable time and load values using time step functions. The maximum total deformation of the robotic arm is 0.319 and the maximum equivalent von-mises stress is 75.455 Pa as shown in the Table 3.5.
- The results show that the robotic arm modeled can withstand various loads.
- In the simulation of robotic arm for arc welding, the joint displacements, torque of the manipulator are shown in Fig 3.3, 3.4 respectively.
- The maximum torque produced to simulate the robotic arm is 0.4 NM and the maximum displacement of robotic arm for arc welding is 0.35 m.
- Maximum electrode displacement for arc welding robotic arm is 0.59 m.
- The maximum displacement of robotic arm for spot-welding is 0.55 m and maximum contact forces between each electrode is 0.85 N.
- With all these loads applied on the robotic arm, the manipulator is still not deformed and the structure can withstand loads that are even higher than these loads.

5 Conclusions and Future scope

A robotic arm is modelled according to the requirement i.e., a roof top fixed robotic arm in industrial sector for reducing workspace of the manipulator using CATIA and the analysis and simulation of the robotic arm is carried out using ADAMS and ANSYS workbench, MATLAB and found out that the design of this robotic arm is possible.

5.1 Future scope

- The design of the robotic arm is a non-linear problem and optimization of robotic arm design can be done.
- Further research can also be done on various robotic manipulators like spot welding, arc welding, assembling robots which are fixed on the roof to reduce the workspace.
- The major benefit of future researcher can carry this work to develop robotic arms for versatile use in industries with various grippers for performing various activities.

References

[1] H. Fleischer, S. Joshi, T. Roddelkopf, M. Klos, and K. Thurow, "Automated Analytical Measurement Processes Using a Dual-Arm Robotic System," *SLAS Technol. Transl. Life Sci. Innov.*, p. 247263031982761, Feb. 2019.

[2] H. EL Daou, K. C. G. Ng, R. Van Arkel, J. R. T. Jeffers, and F. Rodriguez y Baena, "Robotic hip joint testing: Development and experimental protocols," *Med. Eng. Phys.*, vol. 63, pp. 57–62, Jan. 2019.

[3] J. Koivumäki, W.-H. Zhu, and J. Mattila, "Energy-efficient and high-precision control of hydraulic robots," *Control Eng. Pract.*, vol. 85, pp. 176–193, Apr. 2019.

[4] G. L. Cruz, H. Alazki, and R. G. Hernández, "Super Twisting Control For Thermo's Catalyst-5 Robotic Arm," *IFAC-Pap.*, vol. 51, no. 13, pp. 303–308, 2018.

[5] H. Celikag, N. D. Sims, and E. Ozturk, "Cartesian Stiffness Optimization for Serial Arm Robots," *Procedia CIRP*, vol. 77, pp. 566–569, 2018.

[6] J. Oaki, "Physical Parameter Estimation for Feedforward and Feedback Control of a Robot Arm with Elastic Joints," *IFAC-Pap.*, vol. 51, no. 15, pp. 425–430, 2018.

[7] K. Raza, T. A. Khan, and N. Abbas, "Kinematic analysis and geometrical improvement of an industrial robotic arm," *J. King Saud Univ. - Eng. Sci.*, vol. 30, no. 3, pp. 218–223, Jul. 2018.

[8] Mst. N. T. Shanta and N. Z. Azlan, "Function Approximation Technique based Sliding Mode Controller Adaptive Control of Robotic Arm with Time-Varying Uncertainties," *Procedia Comput. Sci.*, vol. 76, pp. 87–94, 2015.

[9] N. Kousi, G. Michalos, S. Aivaliotis, and S. Makris, "An outlook on future assembly systems introducing robotic mobile dual arm workers," *Procedia CIRP*, vol. 72, pp. 33–38, 2018.

[10] S. Pradhan, K. Rajarajan, and A. S. Shetty, "Prototype, emulation, implementation and evaluation of SCARA Robot in industrial environment," *Procedia Comput. Sci.*, vol. 133, pp. 331–337, 2018.

[11] M. Brunot, A. Janot, and F. Carrillo, "State Space Estimation Method for the Identification of an Industrial Robot Arm," *IFAC-Pap.*, vol. 50, no. 1, pp. 9815–9820, Jul. 2017.

[12] D. Busson, R. Bearee, and A. Olabi, "Task-oriented rigidity optimization for 7 DOF redundant manipulators," *IFAC-Pap.*, vol. 50, no. 1, pp. 14588–14593, Jul. 2017.

[13] A. Marwan, M. Simic, and F. Imad, "Calibration method for articulated industrial robots," *Procedia Comput. Sci.*, vol. 112, pp. 1601–1610, 2017.

[14] M. Hamaya, T. Matsubara, T. Noda, T. Teramae, and J. Morimoto, "Learning assistive strategies for exoskeleton robots from user-robot physical interaction," *Pattern Recognit. Lett.*, vol. 99, pp. 67–76, Nov. 2017.

[15] P. Božek, A. Al Akkad M, P. Blištan, and I. Ibrahim N, "Navigation control and stability investigation of a mobile robot based on a hexacopter equipped with an integrated manipulator," *Int. J. Adv. Robot. Syst.*, vol. 14, no. 6, p. 172988141773810, Nov. 2017.

[16] S. Fan, Y. Zhang, Y. Zhang, and Z. Fang, "Motion process monitoring using optical flow–based principal component analysis-independent component analysis method," *Adv. Mech. Eng.*, vol. 9, no. 11, p. 168781401773323, Nov. 2017.

[17] L. Cen and S. N. Melkote, “Effect of Robot Dynamics on the Machining Forces in Robotic Milling,” *Procedia Manuf.*, vol. 10, pp. 486–496, 2017.
[18] Y. Yang *et al.*, “Ultrasonic robotic system for noncontact small object manipulation based on Kinect gesture control,” *Int. J. Adv. Robot. Syst.*, vol. 14, no. 6, p. 172988141773873, Nov. 2017.
[19] S. C. Gutiérrez, R. Zotovic, M. D. Navarro, and M. D. Meseguer, “Design and manufacturing of a prototype of a lightweight robot arm,” *Procedia Manuf.*, vol. 13, pp. 283–290, 2017.
[20] A. Freddi, S. Longhi, A. Monteriù, and D. Ortenzi, “Redundancy analysis of cooperative dual-arm manipulators,” *Int. J. Adv. Robot. Syst.*, vol. 13, no. 5, p. 172988141665775, Sep. 2016.
[21] D. McMorran, D. C. K. Chung, J. Li, M. Muradoglu, O. W. Liew, and T. W. Ng, “Adapting a Low-Cost Selective Compliant Articulated Robotic Arm for Spillage Avoidance,” *J. Lab. Autom.*, vol. 21, no. 6, pp. 799–805, Dec. 2016.
[22] T.-H. S. Li, C.-J. Lin, P.-H. Kuo, and Y.-H. Wang, “Grasping Posture Control Design for a Home Service Robot Using an ABC-Based Adaptive PSO Algorithm,” *Int. J. Adv. Robot. Syst.*, vol. 13, no. 3, p. 118, Jun. 2016.
[23] R. Roy, M. Mahadevappa, and C. S. Kumar, “Trajectory Path Planning of EEG Controlled Robotic Arm Using GA,” *Procedia Comput. Sci.*, vol. 84, pp. 147–151, 2016.
[24] H. Al-Junaid, “ANN Based Robotic Arm Visual Servoing Nonlinear System,” *Procedia Comput. Sci.*, vol. 62, pp. 23–30, 2015.
[25] K. Bouzgou and Z. Ahmed-Foitih, “Workspace Analysis and Geometric Modeling of 6 DOF Fanuc 200IC Robot,” *Procedia - Soc. Behav. Sci.*, vol. 182, pp. 703–709, May 2015.
[26] T. D. Sunny, T. Aparna, P. Neethu, J. Venkateswaran, V. Vishnupriya, and P. S. Vyas, “Robotic Arm with Brain – Computer Interfacing,” *Procedia Technol.*, vol. 24, pp. 1089–1096, 2016.
[27] B. Jobbágy, D. Šimšík, J. Karchňák, and D. Onofrejová, “Robotic Arm with Artificial Muscles in Rehabilitation,” *Procedia Eng.*, vol. 96, pp. 195–202, 2014.
[28] H.-I. Lin, Y.-C. Liu, and Y.-H. Lin, “Intuitive Kinematic Control of a Robot Arm via Human Motion,” *Procedia Eng.*, vol. 79, pp. 411–416, 2014.
[29] A. Gómez-Espinosa *et al.*, “Design and Construction of a Didactic 3-DOF Parallel Links Robot Station with a 1-DOF Gripper,” *J. Appl. Res. Technol.*, vol. 12, no. 3, pp. 435–443, Jun. 2014.
[30] R. Kang, D. T. Branson, E. Guglielmino, and D. G. Caldwell, “Dynamic modeling and control of an octopus inspired multiple continuum arm robot,” *Comput. Math. Appl.*, vol. 64, no. 5, pp. 1004–1016, Sep. 2012.